Modellierung von Gashydraten und deren Wachstumsverhalten im Porenraum mariner Sedimente mit Hilfe der Distinkte Elemente Methode.

Dissertation

zur Erlangung des

Doktorgrades in den Naturwissenschaften

am Fachbereich Geowissenschaften

der Universität Bremen

vorgelegt von

Stefan Kreiter

Bremen, Mai 2007

Betreuer

Prof. Dr. Tobias Mörz

Prof. Dr. -Ing. Volker Feeser

Gutachter

Prof. Dr. Tobias Mörz

Prof. Dr. Katrin Huhn

Kolloquium am 24. 7. 2007

Die Arbeit wurde redaktionell leicht überarbeitet.

Content

Zusammenfassung

Bei vielen größeren Hangrutschungen am Kontinentalrand liegt die Bruchzone in von Gashydrat beeinflußten Sedimenten. Deshalb ist das Verständnis des mechanischen Verhaltens von gashydrathaltigem Sediment ein Schlüsselfaktor, um die Gefährdung der weltweiten Küstengebiete abschätzen zu können. Gashydrathaltige Sedimente sind darüber hinaus als wichtiger Speicher von organischem Kohlenstoff, für die Klimaentwicklung und als potentielle Energie-Ressource interessant.

Im Mittelpunkt der Arbeit steht die Entwicklung einer Technik, die es erlaubt, Gashydratwachstum im Sediment zu simulieren. Dazu wird die Distinkte-Elemente-Methode (DEM) eingesetzt. Die DEM modelliert das Sediment und das sich im Porenraum entwickelnde Gashydrat mit individuellen Partikeln, das unterschiedliche Verhalten entsteht durch grundsätzlich verschiedene Wechselwirkungen zwischen den Partikeln.

Die Oberflächenenergie von Gashydrat bestimmt die Kristallisationskraft der wachsenden Gashydrat-Kristalle. Um die Oberflächenenergie mit Hilfe der DEM zu simulieren, wurde die Standard-DEM um eine mit der Partikelgröße skalierte interne Anziehung erweitert, diese Anziehung entspricht der intermolekularen Anziehung, die der Physik der Oberflächenenergie zugrunde liegt. Zur Beschreibung der Anziehung zwischen den Partikeln wurde das Mie-Potential gewählt, welches den besten Kompromiß zwischen kurzer Reichweite und geringer Steifigkeit darstellt, was eine optimale Nutzung der Rechenleistung erlaubt. Zusätzlich werden die Gashydrat simulierenden Partikel mit zufälligen Bewegungen angeregt, damit Formänderungen möglich sind. Um Kristallwachstum zu simulieren wurden zwei Mechanismen implementiert. Erstens wachsen die das Gashydrat simulierenden Einzel-Partikel bis zu einer Maximalgröße und mit ihnen der simulierte Kristall. Zweitens werden ab der Maximalgröße die Partikel durch drei flächengleiche kleine Partikel ersetzt und diese Partikel wachsen dann weiter. So entsteht eine im Mittel konstante Größenverteilung in dem Partikelcluster und dynamisches Wachstum ist möglich. Diese Methode Gashydratkristallwachstum zu simulieren

wurde theoretisch hergeleitet und mit einer Serie von virtuellen Experimenten auf ihre Anwendbarkeit hin überprüft.

Der Einfluß des Bildungszeitpunkts von Gashydrat im Verlauf einer normalen Sedimentation wurde in einem virtuellen Oedometer gemessen. Oedometer-Versuche messen das Verhalten von Sedimenten unter verschiedenen Auflasten, entsprechend verschiedener Tiefen. Die normale Sedimentation entspricht einer allmählichen Lastzunahme im Oedometer. Einmal wurde das Wachstum von Gashydrat vor der Versenkung und einmal nach der Versenkung simuliert. Dabei ergibt sich zu einen bei Wachstum vor der Versenkung eine stärkere Volumenzuname des Sediments als für Wachstum in größerer Tiefe. Zum anderen ist die Richtung der größten Hauptspannung nach der Versenkung unterschiedlich. Bei frühem, flachen Gashydratwachstum und anschließender Lastzunahme ist sie vertikal ausgerichtet bei spätem Wachstum in der Tiefe, nach der Lastzunahme, ist sie horizontal ausgerichtet.

Gashydrat in natürlichen Sedimenten bildet in Abhängigkeit von der Umgebung teils Zemente, teils Linsen, teils Lagen und teils ist es fein verteilt. Lagenförmige Gashydrate sind manchmal Schichtgebunden, manchmal tritt das Gashydrat auch als lagenförmige Kluftfüllung auf, wann welches Gashydratgefüge auftritt ist jedoch noch nicht verstanden. Um den Einfluß des Sediments auf die Form eines wachsenden Gashydratkristalls zu untersuchen, wurden in Reihe von Experimenten Sedimente mit unterschiedlicher Anisotropie in der Partikel-Ausrichtung und -Länge unter veränderlicher Gesamtspannung untersucht. Sowohl größere Anisotropie in der Partikelausrichtung und größere Normalspannungen begünstigen das Wachstum von Gashydrat in Lagen. Der Endzustand nach dem Gashydratwachstum wird in Zukunft für Experimente zur Festigkeit von gashydrathaltigem Sediment und für Berechnungen der Stabilität von Kontinentalhängen weiter verwendet werden.

Mit einem virtuellen Vorversuch wurde zudem die Möglichkeit aufgezeigt, neben dem Wachstum auch den Zerfall von Gashydrat zu simulieren.

Abstract:

The mechanical behavior of gas hydrate bearing sediment is a possible trigger for huge tsunami-generating slides on continental margins. The mechanical behavior of gas hydrate in the sediment is therefore important for risk assessment in costal areas and may explain major carbon releases in the geological past. Gas hydrate is a potential future energy source and the mechanical behavior of gas hydrate bearing sediment is crucial for the exploration and exploitation of this energy source, but little is known of gas hydrates mechanical behavior in sediment. Also the different fabrics of natural gas hydrate are only partly understood. Here a method is proposed to simulate the behavior of gas hydrate in sediment on the pore scale using the Distinct Element Method (DEM).

The simulation is founded on the surface energy, which is the cause for the forces exerted by growing crystals. The simulation uses attractive particle interaction and random particle agitation to generate a surface tensed material. This material behaves like gas hydrate in terms of surface tension and forces to the neighboring sediment. The behavior of this gas hydrate simulating material has been calibrated and validated by a series of different experiments.

The influence of early and late gas hydrate growth during normal sedimentation is tested in a virtual one dimensional compression test (oedometer). The main difference between early and late growth lies in the final orientation of the main principal stress direction.

The influence of the host sediment on gas hydrate fabric is tested by a series of growth experiments in different virtual host sediments under different stress states. Samples with low anisotropy and low confining stress lead to nodular growth of gas hydrate while highly anisotropic host sediments lead to layered or vein like growth. The virtual sediment with the final fabric will be used as starting point for future experiments regarding shear strength of gas hydrate bearing sediments and continental slope stability.

In a preliminary experiment the simulation of gas hydrate decay was demonstrated.

1. Introduction

Gas hydrate research is embracing three of the most important issues in geosciences: natural hazards, energy supply and climate change. It is fascinating to work on an exotic substance which is unstable under earth surface conditions, but is a common component of deeper lying sediments. Another interesting feature of natural gas hydrate is that it is always near to the phase boundary.

An introduction to gas hydrate research with a focus to slope stability and gas hydrate fabric is given in the following section. The introduction is followed by background information regarding the organization, the context and the motivation of the study. Finally a draft of the PhD project is given to introduce the three manuscripts.

1.1 History of gas hydrate research

The first artificially produced gas hydrates were reported by Davy (Davy, 1811). This discovery was followed by the study of the stoichiometry of different artificial hydrate compositions. Over the time more molecules were discovered which form gas hydrates. Methane hydrate and hydrates of other hydrocarbons were described first by Villard (Sloan, 1998; Villard, 1888). The identification of the gas hydrate structure was accomplished at the University of Bonn (v. Stackelberg, 1949; v. Stackelberg and Müller, 1954).

The next phase of research rose from the practical importance of gas hydrates for the oil industry in the 1930's. Gas hydrates form at the valves of pipelines from natural gases and water and frequently block the gas flow. In order to prevent this, methods to inhibit gas hydrate growth were developed. As a result gas hydrate research was mainly concerned with thermodynamics and kinetics (Sloan, 1998).

The importance of gas hydrate research was fully realized after their discovery in nature. Natural gas hydrates were first discovered in the permafrost regions of Siberia in 1969, then

independently in Alaska in 1972. The discovery of gas hydrate in the seafloor was made during the Deep Sea Drilling Project (DSDP). From there on gas hydrates were recognized as an important part of the global carbon cycle and as an important factor for the climate. Recently gas hydrates are explored as a potential exotic energy resource (Collett, 2002).

1.2 Chemistry and structure of gas hydrates

Gas hydrates are crystalline solids containing water and hydrophobic molecules. The water molecules form a hydrogen bonded-three-dimensional lattice, the molecules are located in cavities which they stabilize by their hydrophobic interaction (fig. 1). Over 130 different molecules crystallize as hydrates in three different crystalline structures (I, II, H). All hydrate structures have at least two types of cavities. The structures I and II have a cubic crystal symmetry, H is hexagonal (Sloan, 1998).

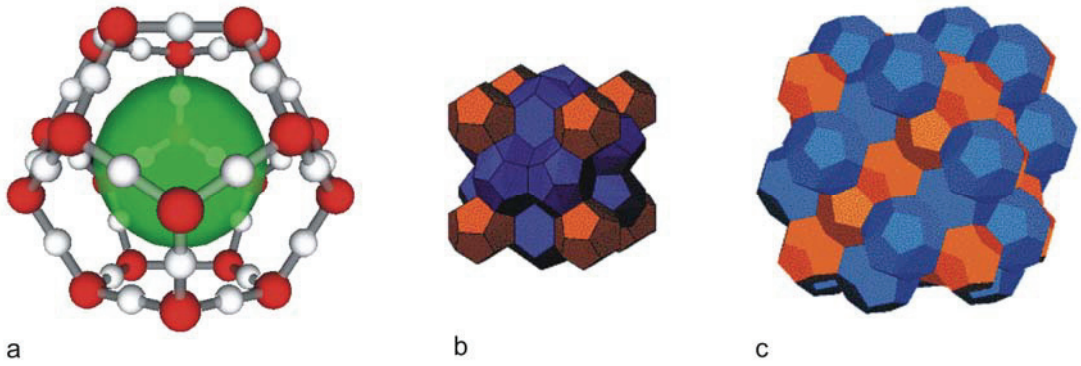

Figure 1.: Structure of gas hydrates; a) pentagonal dodecahedron formed by water, red oxygen, white hydrogen, green rotating hydrophobic molecule. b) Unit cell of structure I gas hydrate e. g. 8 CH_4 46 H_2O, orange pentagonal dodecahedrons, blue Hexakaidecahedrons c) Unit cell of structure II gas hydrate e. g. 8 C_2H_6 16 CH_4 136 H_2O, orange pentagonal dodecahedrons, blue Hexakaidecahedrons. Pictures modified from (Webber, 2002) (a) and (Rawn, 2004) (b,c).

In nature, methane hydrate is the most common gas hydrate. Pure methane hydrate has the crystal structure of I, but hydrates of mixtures of higher hydrocarbons and methane exist which crystallize in structure II and H. The methane sources are biological degradation of biomass by methane-producing micro organisms or thermal decomposition of biomass. Higher order

hydrocarbons originate from thermal decomposition and frequently occur above oil and gas fields.

1.3 Natural gas hydrates

1.3.1 Gas hydrate fabric in natural sediments

Natural gas hydrates have been sampled in many locations around the world. Since most of the samples were taken with standard sampling equipment, the cores were subjected to lower pressures and higher temperatures, outside the stability field of gas hydrate before the further processing. During ODP leg 164, the first leg dedicated to gas hydrates, most of the gas hydrate occurrences where inferred from pore water freshening and soupy sediment consistence (Shipboard Scientific Party, 1996). Therefore the fabric of the gas hydrate in the sediment could only be observed for massive gas hydrate occurrences.

By far the best gas hydrate fabric samples have been taken from pressurized cores, which have been imaged by computer tomography scans (Abegg et al., 2007; Abegg et al., 2006; Abegg et al., 2003).

Natural gas hydrates in sediments have been found in various fabrics: cements, nodules, veins and layers are common and there is evidence for finely disseminated gas hydrates in sediments (Abegg et al., 2006; Abegg et al., 2003; Booth et al., 1998; Ivanov et al., 1998).

The fabric of gas hydrate in sediments is a key factor to understand and predict the behavior of gas hydrate bearing sediment. Most of the geophysical measurements like electrical resistivity (Spangenberg, 2001) or p and s wave velocity (Korenaga et al., 1997) depend on the fabric. So the multitude of possible gas hydrate fabrics poses a major problem for geophysical data interpretation.

Slope stability calculations must make assumptions about the gas hydrate fabric to get reliable results and future gas hydrate exploitation processes are fabric dependent.

1.3.2 Explanations for the natural gas hydrate fabric

One step to explain the multitude of different gas hydrate fabrics found in nature was to link the thermodynamic quantity of surface energy to the geometry of the sediment pores (Clennell et al., 1999; Clennell et al., 1995; Henry et al., 1999). The pore geometry was than linked to grain size (Ginsburg et al., 2000) and experiments have proven the pore size dependent behavior of gas hydrate (Tohidi et al., 2001). A next step was to couple the surface energy to local sediment failure (Feeser, 1997). Other attempts to explain the fabric of natural gas hydrate, focus on the importance of the stress state. Especially the overburden stress was used to explain the succession of gas hydrate fabric found in boreholes (Milkov and Xu, 2005; Torres et al., 2004; Torres et al., 2005).

1.3.4 Gas hydrate stability in natural sediments

Natural gas hydrate occurrences are explored with seismic methods and confirmed by deep sea drilling. Seismic profiles show often a so called BSR (Bottom Simulating Reflector) at active and passive continental margins. Regionally the BSR follows the sediment surface with a constant depth offset and sometimes crosses other structures like bedding (therefore bottom simulating). In contrast to the seafloor reflector the BSR polarity is negative. The BSR results from gas in the pore space below the stability field of gas hydrates (Singh et al., 1993). As confirmed by drilling it is a reliable indicator for gas hydrates. The existence of a BSR indicates the existence of gas hydrates in vast areas of the world wide continental slopes. Drillings on the outer Bahama Rise, however, showed that gas hydrates may also occur in cases where no BSR has been detected (Paull and Matsumoto, 2000).

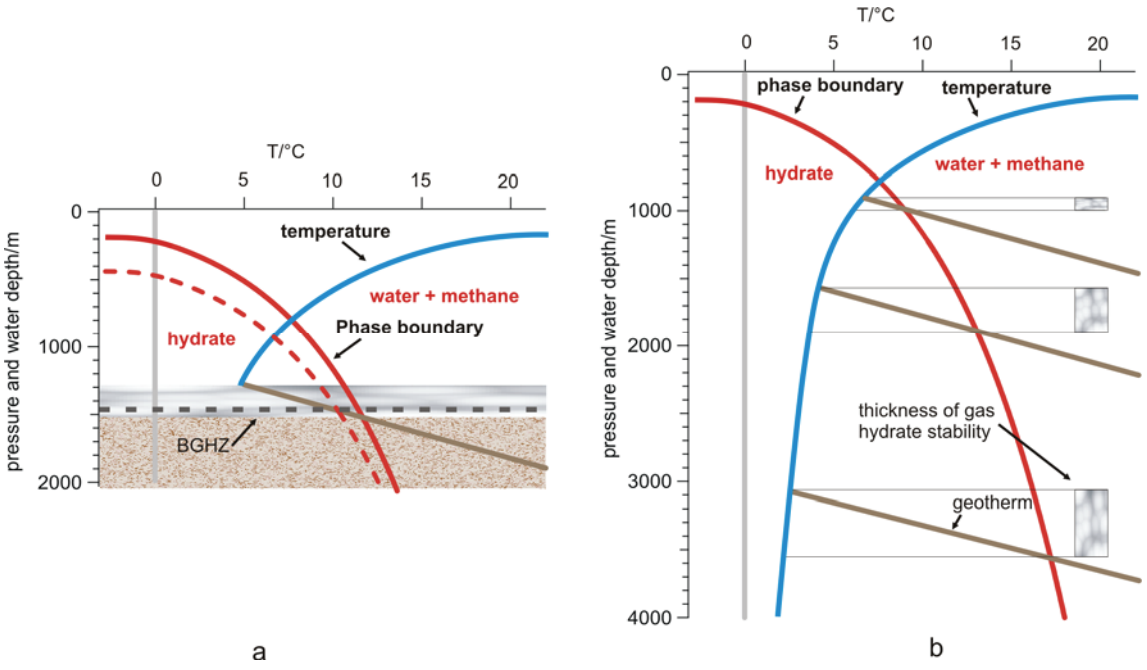

Fig. 2: Phase diagram of methane hydrate combined with a section of the ocean and the seafloor after (Kvenvolden, 1988), pressure converted in equivalent water depth. Red: phase boundary, blue: water temperature, brown: sediment temperature.

a) Vertical section through water and sediment, gray: methane hydrate stable in the sediment, brown: methane hydrate not stable in the sediment. Red dotted: phase boundary of methane hydrate shifted by pressure reduction, gray dotted: new base of methane hydrate stability (BGHZ) in the sediment.

b) Same phase diagram as a), showing the thickness of the gas hydrate stability zone for different seafloor depth. The thickness of the gas hydrate stability zone is indicated.

Gas hydrates are only stable under high pressure and at low temperatures. The phase diagram (fig. 2a) shows where gas hydrates are stable below the seafloor. The temperature in the sediment section is determined by the water temperature at the seafloor and the geothermal gradient caused by heat flow from the interior of the earth. As a consequence methane hydrate is only stable in the uppermost sediment layer. In figure 2b it is illustrated how the zone of gas hydrate stability becomes thicker with increasing depth of the seafloor, the geothermal gradient is plotted for three different water depths.

Apart from pressure and temperature there are other factors which affect the stability of methane hydrate, an important one being the size of the sediment pores. In very small pores the surface energy for the formation of the gas hydrate crystals is so large that the stability field of gas hydrate is shifted to distinctly higher pressure or lower temperatures (Clennell et al., 1999;

Clennell et al., 1995; Feeser, 1997; Henry et al., 1999). Substances which are dissolved in the water affect the stability of gas hydrate as well, salt e.g. hinders the hydrate formation, similar to the hindered formation of ice in salt water (Sloan, 1998).

There are four important processes that lead to the decay of the gas hydrate in the sediment.

1.- A drop of the global sea level lowers the water pressure in the sediment and the base of the gas hydrate stability zone (BGHZ) moves upward, as suggested in fig. 1a.

2.- A sediment package raised by local tectonics suffers regionally a similar destabilization of the gas hydrates.

3.- A long lasting warming of the bottom water temperature, e.g. by a change in the global current system, leads to a rise of the BGHZ (Kennett et al., 2003). Note that it takes a long time until the heat pulse has reached the BGHZ (Milkov and Sassen, 2003).

4.- Normal sedimentation leads also to a rise of the BGHZ, because the increasing thermal isolation leads to higher temperatures from the intake of the terrestrial heat.

1.3.5 Gas hydrate, climate history and the carbon cycle

If larger amounts of methane are released from gas hydrate, it has a severe impact on the climate. Unaltered methane in the atmosphere is a 32-fold stronger greenhouse gas than CO_2. Even if the carbon released form the gas hydrates enters the atmosphere in the oxidized form of CO_2, the huge amount of carbon which is stored in gas hydrates is of potential relevance for the climate. The processes, which transport the carbon form the deep marine sediments to the atmosphere, are not well constrained; explosive gas discharge and submarine slides seem to be the most probable processes.

Kennett et al. (2003), argued for a strong involvement of gas hydrate in the carbon cycle during the last ice ages. He analyzed the methane records from the polar ice cores and showed that peatlands were not well enough developed to explain the methane concentration patterns. He

concluded that it is most likely that methane from gas hydrate was released during the deglaciation periods. He proposed a warming of the intermediate waters as agent for the release of gas hydrate by triggering submarine slides. But this link between climate and gas hydrate driven submarine slides is highly debated (Hanson, 2004; Kennett et al., 2003; Maslin et al., 2004).

Several distinct climatic events in the past have also been attributed to gas hydrate release. The Paleocene - Eocene climatic optimum is a warm phase probably generated by gas hydrate decay (Dickens et al., 1997; Farley and Eltgroth, 2003; Katz et al., 1999; Thomas et al., 2002). Another big gas hydrate release event took place in the Jurassic causing an oceanic anoxic event (Hesselbo et al., 2000). At the end of the Permian, the largest mass extinction ever, was probably also caused by an extreme release of methane from gas hydrates (Hanson, 2004; Stokstad, 2003)

1.3.6 Gas hydrate as energy resource

The estimates of methane stored in form of gas hydrate vary widely, but agree, that ten to hundred times more than the world known classic hydrocarbon reserves are stored in the from of gas hydrate (Kvenvolden and Lorenson, 2001). Countries without sufficient own hydrocarbon reservoirs and countries with exaggerated energy consumption (Japan, India, USA) hope that they can dissolve the gas hydrate in the underground and exploit the methane stored in gas hydrates in their continental margins (Collett, 2002).

One production test was conducted at the Mackenzie delta in northern Canada (Dallimore et al., 2004). However the feasibility of an economic industrial exploitation remains unclear (Collett, 2002).

Because CO_2 builds also hydrate, there exist plans to store the CO_2 from human fossil fuel consumption in the form of CO_2 gas hydrate on or in the deep sea floor (Lee et al., 2003).

1.3.7 Gas hydrate and Slope stability

McIver was the first to postulate that gas hydrates may trigger submarine slides (McIver, 1982). Since then a number of slope failures have been attributed to gas hydrates (Bondevik et al., 2002; Bondevik et al., 1997; Kayen and Lee, 1993) and table 6 in chapter 9 of Kennett et al. (2003).

Two processes have been proposed by which gas hydrate may destabilize a slope: the first is that the growth of gas hydrate stops the normal consolidation and leaves after its disappearance a very soft sediment behind, which forms a potential failure plane. The second process is that the volume increase during rapid gas hydrate decay lowers the effective stress to such an extent, that slope failure occurs. Which process takes place in nature is not known. The arguments to attribute the slope failures to gas hydrate decay, are mostly the geometric coincidence of the failure plane with the seismic BSR. Figure 3 shows a multichannel seismic line perpendicular to the Costa Rica continental margin, showing a clear BSR and a slide where the BSR crosses the sediment surface. The slide was discovered by Christian Müller and presented during a status seminar (Müller et al., 2007; Müller et al., 2002).

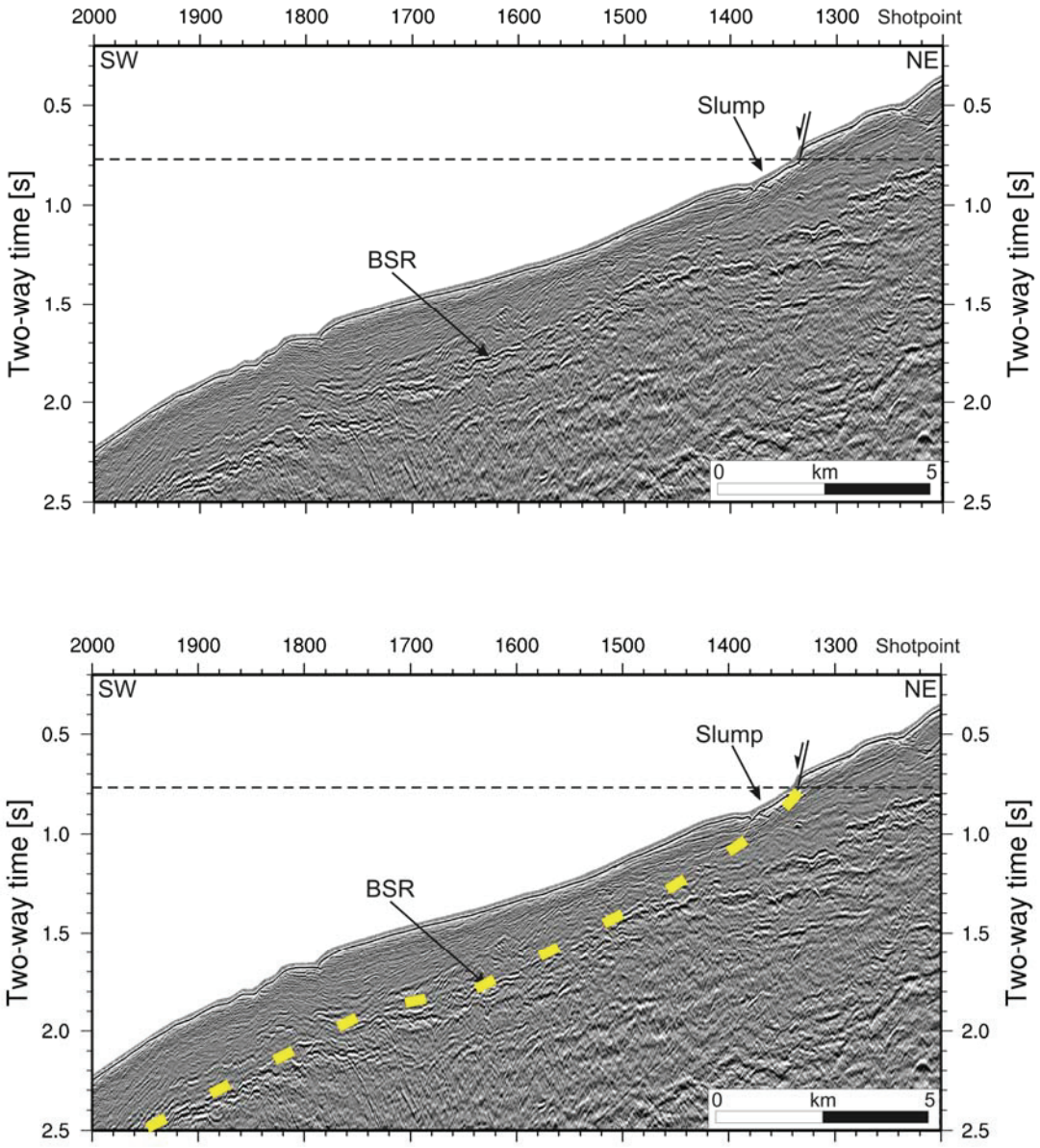

Figure 3: Seismic section of the Costa Rica continental margin across BGR slide, black dashed line: upper boundary of gas hydrate stability in the water. Yellow dashed line in the lower part: location of the bottom simulating reflector (BSR) seismics by C. Müller (Müller et al., 2007)

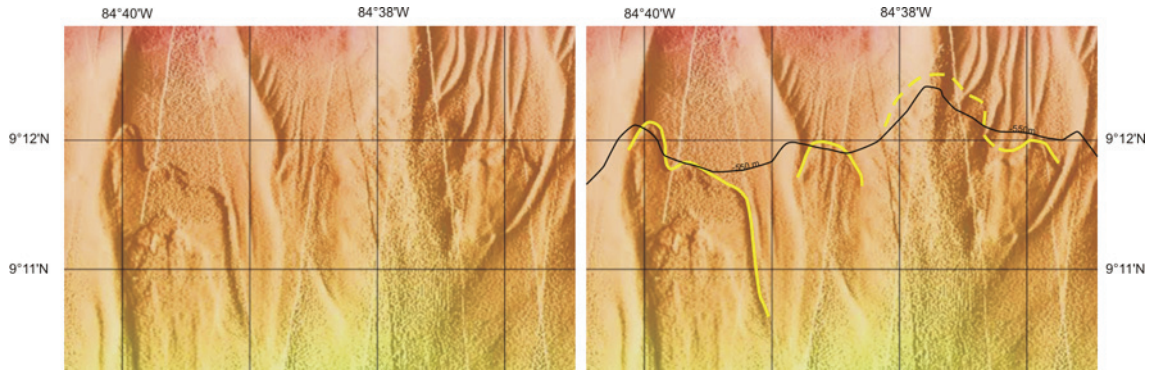

Figure 4: Bathymetric map of the BGR and GEOMAR slides, left shaded bathymetric rainbow plot. Right: Same plot with -550 m isobathic line, the head scarps of the mass slides are indicated by yellow lines, dashed is assumed. Bathymetry magnified from (Bialas, 2004), isobathic line combined from (Klaucke et al., 2004).

The head scarps and the moved material of the BGR slide of two other slides is also seen on the bathymetric maps of Figure 4. It can be seen that the head scarps are all aligned around the 550 m isobathic line, the depth where the gas hydrate stability zone crosses the seafloor. These two geometric arguments suggest strongly, that the outcrop of the base of the gas hydrate stability zone played a role during the generation of these slides. A similar convincing relationship was established e.g. for the northern Alaskan margin (Kayen and Lee, 1993), but the actual link between gas hydrates and the slides remains speculative.

There exist a number of papers which calculate the movement of the gas hydrate stability zone in the sediment and give thermodynamic constraints to gas hydrate accumulation and dissolution, some of which claim the importance of gas hydrate decay for slope failures (Davie et al., 2004; Delisle et al., 1998; Egeberg and Dickens, 1999; Gering, 2003; Gorman et al., 2002; McIver, 1982; Mienert et al., 2001; Milkov and Sassen, 2003; Riestenberg et al., 2003; Zatsepina and Buffett, 1998), but in none of these papers the stability of a slope is actually calculated. Only two conference papers and one journal article (Hovland et al., 2001; Sultan et al., 2004; Sultan et al., 2003) try to assess slope stability. There the gas hydrates influence is only modeled as an additional source of pore pressure, in Sultan et al. (2004) it is clearly stated that the "degradation of the soil resistance due to hydrate melting has not been investigated in literature and consequently was unfortunately not considered correctly in this study". To

conclude, the mechanical behavior of gas hydrate bearing sediment is an unsolved question and a new interesting field of research.

2. Development and concept of the study

2.1 The GASSTAB project

The concept of this study was outlined in the middle phase of the joint project "GASSTAB" (Standsicherheit und Stabilität gashydratführender Tiefseehänge und Meeresböden) in 2002. The aim of the GASSTAB Project was to investigate the influence of gas hydrates on the slope stability at the continental margins. GASSTAB consisted of three working groups: An experimental working group developed a test system for gas hydrate bearing sediments at the University of Kiel, led by Prof. Dr. -Ing. Feeser. A civil engineering group from the TU Berlin, lead by Prof. Dr. -Ing. S. Savidis set up a slope model capable of dynamic calculation and simulated the impact of earthquakes on the continental slope stability. The AG WUM (Wasser-, Umwelt-, Meeres-Forschung/-Technik) lead by B. Grupe, worked mainly on the sedimentologic characterization of gas hydrate host sediments. The AG WUM was located at the independent research institute VWS (Versuchsanstalt für Wasser und Schiffbau), and was only recently associated with the TU-Berlin. The AG WUM did no teaching and was not a faculty member. I was member of the AG WUM.

The working group WUM was responsible for the study of the microstructure, mineralogy and grain size of gas hydrate bearing sediments from the Blake Ridge, a famous ODP gas hydrate drilling site (Shipboard Scientific Party, 1996). The main task was the development of a synthetic standard gas hydrate host sediment for the experimental working group. In addition it was planned in the first place to setup a flume experiment for slope stability tests.

In the course of the project it turned out that the flume experiments were underfinanced and seemed not very promising, so the experimental working group in Kiel proposed to set up a

virtual equivalent of their test system with the DEM method. This was the starting point for this thesis, since thereafter I started to develop a virtual oedometric element test for gas hydrate growth experiments.

In addition to the described working program AG WUM was invited by the SFB 574 to participate in two cruises to the Costa Rica continental margin (Flueh et al., 2004; Söding et al., 2003). The AG WUM proposed to explore and sample the BGR slide further, which resulted in the bathymetric map of figure 4 and the discovery of two additional slides during the mapping legs of the cruises. During these cruises two samples of gas hydrate were recovered (Moerz et al., 2003; Moerz et al., 2005; Moerz et al., 2007; Schmidt et al., 2005).

2.2 Motivation for the gas hydrate simulation

It was agreed that the entire project could benefit from a computer simulation of the gas hydrate in the pore space. The ultimate aim of this simulation would be a virtual equivalent for all naturally occurring gas hydrate bearing sediments and the ability to test these virtual samples under arbitrary changes of stress state, temperature, methane concentration or pore water chemistry. Together with laboratory experiments and field measurements this ideal scenario would allow to predict the reactions of any continental slope for a wide scenario of tectonic, climatic or antropogenetic changes. Just some established sediment parameters like the mineralogy, grain size and geophysical field data would than suffice as input.

This ideal model would be an effective tool for natural hazard assessment and would be valuable for the development of gas hydrate exploration and exploitation techniques. It would also contribute to the questions of the role of gas hydrate in the climate history and during mass extinction events and allow to understand the formation history of a gas hydrate bearing sediment just by looking at its fabric.

More realistic goals are to prove the applicability of the simulation by providing data that can be compared to laboratory tests with a well know, easy to simulate material, in which gas hydrate

growth is taking place. Another goal is to simulate a fabric equivalent to fabrics found in nature. Finally a first prediction of shear strength of a gas hydrate bearing material is a realistic aim.

2.3 The Distinct Element Method (DEM)

Since the end of the 70's the Distinct Element Method (DEM) has been used to simulate the characteristics of granular materials as granite rock or loose sand (Cundall and Strack, 1979). Whereas the conventional simulation methods (Finite Elements, Finite Differences or Boundary Elements) transfer only well-known behavior from simple geometry to complex geometry, the DEM can be used to identify the processes in the material. The DEM resembles Molecular Dynamics (MD) simulations (Hobbs et al., 2004), which explain complex phenomena from simple interaction rules e.g. in colloid science and biochemistry.

Distinct Element Models are based on freely moving particles which mutually interact. The movement is governed by Newton's laws of motion and the particle interaction forces are dynamically modeled in time steps. Gravity, rigid walls, unbreakable bonds, bonds with a given strength and other boundary conditions are used to implement a specific model setup. This micro interactions needed as input for the DEM simulation are either known physical properties or are calibrated with the outcome of numerical experiments. The particle behavior in the simulated material is adapted in such a way that numerical experiment and a real experiment show comparable behavior. The standard grain characteristics are density, stiffness and grain friction. But the particle properties can be extended very flexibly to suit to further physical processes. So far e.g. the apparent cohesion produced by water menisci (Gröger et al., 2003) and the complex interactions of clay minerals were added to the DEM simulation (Yao and Anandarajah, 2003). Problems which cannot be solved with conventional methods, like the propagation of cracks and their acoustic emission can be realistically predicted (Akoi et al., 2004). Also dynamic processes like the transfer of toner in a laser printer or ore separation processes have been simulated with the DEM (Kawamoto, 2004; Murariu et al., 2004).

2.4 The course of the project

The DEM was completely new to the working group. The commercial framework "particle flow code" PFC^{2D} (Itasca Consulting Group, 2002) was used during the study. A first very preliminary implementation of growing of single element was presented in 2002 (Grupe et al., 2002). The code was improved adding element decay and the addition of a first simple linear attractive potential with attraction and cut off like the one used by Kadau (Kadau et al., 2001); this was presented during a workshop in 2002 (Kreiter et al., 2002).

A complete redesign of code was necessary to eliminate the n-square scaling problem of the neighbor detection from the simulation (Allen and Tildesley, 1987). The effective contact detection routine from PFC^{2D} can only be accessed via the C++ extension while the first simulation was implemented in the proprietary scripting language called "fish".

An analysis of the stress evolution during the growth of a surface tensed phase in a granular material was presented in 2003 (Kreiter and Feeser, 2003). The simulation was extended further alongside to the other project work with a preliminary implementation of hydrate decay and a first theoretical connection between surface tension and the attractive particle interaction was established during the final phase and shortly after the end of the GASSTAB project (Kreiter et al., 2004).

2.5 Extension of the simulation in Bremen

After the end of the GASSTAB project, I got the possibility to join the new working group of Tobias Mörz in Bremen and to refine the results from GASSTAB to this PhD thesis. The work regarding the simulation was focused in a first phase on the theoretical proof and quantitative calibration of the implementation of surface tension in the DEM simulation (Kreiter et al., 2007a).

Following this step the attention was focused on the host sediment - gas hydrate interaction, with the goal to reproduce the natural fabrics of gas hydrate found in marine sediment samples. Gas hydrate was grown in several types of virtual sediment with different anisotropies and stress states and the resulting fabric were quantified (Kreiter et al., in prep.). First results of the fabric simulation were also presented at the EGU meeting in Wien 2007 (Kreiter et al., 2007b).

Now the cumulative part of the thesis follows with the peer reviewed and published papers (Kreiter et al., 2004; Kreiter et al., 2007a) and the manuscript (Kreiter et al., in prep.).

References

Abegg, F., Bohrmann, G., Freitag, J. and Kuhs, W.F., 2007. Fabric of gas hydrate in sediments from Hydrate Ridge—results from ODP Leg 204 samples. Geo-Marine Letters, 27(2): 269-277.

Abegg, F., Bohrmann, G. and Kuhs, W.F. (Editors), 2006. Data report: Shapes and structures of gas hydrates imaged by computed tomographic analyses, ODP Leg 204, Hydrate Ridge. Proceedings ODP, Scientific Results, 2006, Online, 11 pp.

Abegg, F. et al., 2003. Free gas bubbles in the hydrate stability zone: evidence from CT investigation under in situ conditions, EGS-AGU-EUG Joint Assemly. Geophysical Research Abstracts, Nice, France.

Akoi, K., Mito, Y., Mori, T. and Maejima, T., 2004. Evaluation of behavior of EDZ around rock cavern by AE measurements and PFC simulation. In: Y. Shimizu, R. Hart and P.A. Cundall (Editors), Numerical Modeling in Micromechanics via Particle Methods - 2004. A. A. Balkema, Leiden, pp. 73-83.

Allen, M.P. and Tildesley, D.J., 1987. Computer simulation of liquids. Oxford University Press.

Bialas, J., 2004. 6.1 Hydroacoustic Work - Multibeam Swathmapping. In: E. Flueh, E. Söding, E. Suess and K. Wallmann (Editors), RV-Sonne Cruise Report SO173/1,3&4. Subduction II: The Central American Continental Margin. GEOMAR report 115, Kiel.

Bondevik, S. et al., 2002. The Storegga Slide tsunami along the Norwegian coast - from the geological record to numerical simulations.

Bondevik, S., Svendsen, J.I., Johnsen, G., Mangerud, J. and Kaland, P.E., 1997. The Storrega tsunami along the norwegian coast, its age and runup. Boreas, 26: 29-53.

Booth, J.S., Winters, W.J., Dillon, W.P., Clennell, M.B. and Rowe, M.M., 1998. Major occurrences and reservoir concepts of marine clathrate hydrates: implications and field evidence. In: J.P. Henriet and J. Mienert (Editors), Gas hydrates; relevance to world margin stability and climate change. Geological Society Special Publications. Geological Society of London, London, United Kingdom, pp. 275-291.

Clennell, M.B., Hovland, M., Booth, J.S., Henry, P. and Winters, W.J., 1999. Formation of natural gas hydrates in marine sediments 1. Conceptual model of gas hydrate growth conditioned by host sediment properties. Journal of Geophysical Research, 104(B10): 22985-23003.

Clennell, M.B., Hovland, M., Lysne, D. and Booth, J.S., 1995. Role of capillary forces, coupled flows and sediment-water depletion in the habit of gas hydrate. EOS, 76(17, supplement): 164-165.

Collett, T.S., 2002. Energy Resource Potential of Natural Gas Hydrates. AAPG Bulletin, 86(11): 1971-1992.

Cundall, P.A. and Strack, O.D.L., 1979. A Discrete Numerical Model for Granular Assemblies. Géotechnique, 29: 47-65.

Dallimore, S.R., Uchida, T. and Collett Timothy, S. (Editors), 2004. Scientific results from JAPEX/JNOC/GSC Mallik 2L-38 gas hydrate research well, Mackenzie Delta, Northwest Territories, Canada. Geological Survey Canada Bulletin, 544.

Davie, M.K., Zatsepina, O.Y. and Buffett, B.A., 2004. Methane solubility in marine hydrate environments. Marine Geology, 203(1-2): 177-184.

Davy, H., 1811. On a combination of oxymuratic gas and oxygene gas (from Sloan 1998). Royal Society of London Philosophical Transactions, 101: 155-162.

Delisle, G., Beiersdorf, H., Neben, S. and Steinmann, D., 1998. The geothermal field of the Norht Sulawesi accretionary wedge and a model on BSR mirgration in unstable despositional enviroments. In: H.J. P. and J. Mienert (Editors), Gas Hydrates: Relevance to World Margin Stability and Climate Change. Special Publications. Geological Society, London, pp. 267-274.

Dickens, G.R., Castillo, M.M. and Walker, J.C.G., 1997. A blast of gas in the latest Paleocene: Simulating first-order effects of massive dissociation of oceanic methane hydrate. Geology, 25(no.3): 259-262.

Egeberg, P.K. and Dickens, G.R., 1999. Themodynamic and pore water halogen constraints on gas hydrate distribution at ODP Site 997 (Blake Ridge). Chemical Geology, 153: 53-79.

Farley, K.A. and Eltgroth, S.F., 2003. An alternative age model for the Paleocene-Eocene thermal maximum using extraterrestrial (super 3) He. Earth and Planetary Science Letters, 208(3-4): 135-148.

Feeser, V., 1997. Gashydratbildung in Tiefseesedimenten - Zur Rolle der sedimentmechanischen Prozess-Steuereung. DGMK-Tagungsbericht, 9706: 51-60.

Flueh, E., Söding, E., Suess, E. and Wallmann, K. (Editors), 2004. RV-Sonne Cruise Report SO173/1,3&4. Subduction II: The Central American Continental Margin, 115. GEOMAR report 115, Kiel.

Gering, K.L., 2003. Simulations of methane hydrate phenomena over geologic timescales; Part I, Effect of sediment compaction rates on methane hydrate and free gas accumulations. Earth and Planetary Science Letters, 206(1-2): 65-81.

Ginsburg, G., Soloviev, V.A., Matveeva, T. and Andreeva, I., 2000. SEDIMENT GRAIN-SIZE CONTROL ON GAS HYDRATE PRESENCE, SITES 994, 995 AND 997. In: K. Paull Charles, R. Matsumoto, J. Wallace Paul and W.P. Dillon (Editors), Proceedings of the Ocean Drilling Program, Scientific Results, pp. 237-245.

Gorman, A.R. et al., 2002. Migration of methane gas though the hydrate stability zone in a low-flux hydrate province. Geology, 30(4): 327-330.

Gröger, T., Tüzün, U. and Heyes, D.M., 2003. Shearing of wet particle systems - discrete element simulation. In: H. Konietzky (Editor), Numerical Modeling in Micromechanics via Particle Methods. A. A. Balkema Publishers, Leiden, pp. 65-72.

Grupe, B. et al., 2002. Slope Stability and Land Slides in the Deep Sea: Influence Parameter Gas Hydrates (GASSTAB). In: A. Rudloff and L. Stroink (Editors), Gas Hydrates in the Geosystem - Status Seminar. GEOTECHNOLOGIEN Science Report No. 1. Koordinierungsbüro GEOTECHNOLOGIEN, Kiel, Germany, pp. 46-48.

Hanson, B., 2004. Editors' Choice: Highlights of the recent literature. GEOLOGY: Rapid Decompression. Science, 303 Nr. 5657(23. 01. 2004).

Henry, P., Michel, T. and Clennell, M.B., 1999. Formation of natural gas hydrates in marine sediments 2. Thermodynamic calculations of stability conditions in porous sediments. Journal of Geophysical Research, 104(B10): 23005-23022.

Hesselbo, S.P. et al., 2000. Massive dissociation of gas hydrate during a Jurassic oceanic anoxic event. Nature (London), 406(6794): 392-395.

Hobbs, B.E. et al., 2004. Ab initio emergent phenomena in PFC. In: Y. Shimizu, R. Hart and P.A. Cundall (Editors), Numerical Modeling in Micromechanics via Particle Methods - 2004. A. A. Balkema Publishers, Leiden, pp. 191-197.

Hovland, M., Orange, D., Bjorkum, P.A. and Gudmestad, O.T., 2001. Gas hydrate and seeps-effects on slope stability; the "hydraulic model". In: S. Chung Jin, M. Sayed, H. Saeki and T. Setoguchi (Editors), The proceedings of the Eleventh (2001) international offshore and polar engineering conference. International Society of Offshore and Polar Engineers. Golden, CO, United States. 2001.

Itasca Consulting Group, I., 2002. PFC^{2D} Particle Flow Code in 2 Dimensions (Version 3.0 Manual). ICG, Minneapolis.

Ivanov, M.K., Limonov, A.F. and Woodside, J.M., 1998. Extensive deep fluid flux through the sea floor on the Crimean continental margin (Black Sea). In: J.P. Henriet and J. Mienert (Editors), Gas hydrates; relevance to world margin stability and climate change. Geological Society Special Publications. Geological Society of London, London, United Kingdom, pp. 195-213.

Kadau, D., Bartels, G., Brendel, L. and Wolf, D.E., 2001. Contact Dynamics Simulations of Compacting Cohesive Granular Systems. Computer Physics Communications.

Katz, M.E., Pak, D.K., Dickens Gerald, R. and Miller, K.G., 1999. The source and fate of massive carbon input during the latest Paleocene thermal maximum. Science, 286: 1531-1533.

Kawamoto, H., 2004. Introduction of reasearch and development on electromechanics of electromagnetic particles for imaging technology. In: Y. Shimizu, R. Hart and P.A. Cundall (Editors), Numerical Modeling in Micromechanics via Paricle Methods - 2004. A.A. Balkema Publishers, Leiden, pp. 95-101.

Kayen, R.E. and Lee, H.J., 1993. Slope stability in regions of sea-floor gas hydrate; Beaufort Sea continental slope. In: W.C. Schwab, H.J. Lee and D.C. Twichell (Editors), Submarine landslides; selected studies in the U.S. Exclusive Economic Zone. U. S. Geological Survey Bulletin. U. S. Geological Survey, Reston, VA, United States, pp. 97-103.

Kennett, J.P., Cannariato, K.G., Hendy, I.L. and Behl, R.J., 2003. Methane Hydrates in Quaternary Climate Change: The Clathrate Gun Hypothesis. AGU Special Publication, 54. AGU, Washington, 216 pp.

Klaucke, I. et al., 2004. 6.2 Deep Tow Acoustic and Seismic Investigations. In: E. Flueh, E. Söding, E. Suess and K. Wallmann (Editors), RV-Sonne Cruise Report SO173/1,3&4. Subduction II: The Central American Continental Margin. GEOMAR report 115, Kiel.

Korenaga, J., Holbrook, W.S., Singh, S.C. and Minshull, T.A., 1997. Natural gas hydrates on the southeast U. S. margin: Constraints from full waveform and travel time inversions of wide-angle seismic data. Journal of Geophysical Research, 102(B7): 15345-15365.

Kreiter, S. and Feeser, V., 2003. Mechanics of growing gas hydrates in marine sediments - Numerical simulation of sediment-hydrate interaction, 14. Tagung für Ingenieurgeologie. Proceedings of the 14th Conference on Engineering Geology, Kiel, Germany, pp. 27-32.

Kreiter, S., Feeser, V. and Grupe, B., 2002. Gashydrate in marinen Sedimenten - Numerische Modellierung der Bildungs- und Rückbildungsprozesse, 4. Workshop - Porous Media, Blaubeuren, Germany.

Kreiter, S., Feeser, V. and Grupe, B., 2004. Numerical simulation of gas hydrate behavior in marine sediments using PFC^{2D}. In: Y. Shimizu, R. Hart and P.A. Cundall (Editors), Numerical Modeling in Micromechanics via Particle Methods - 2004. A. A. Balkema Publishers, Leiden, pp. 191-197.

Kreiter, S., Feeser, V., Kreiter, M., Moerz, T. and Grupe, B., 2007a. A Distinct Element simulation including surface tension - towards the modeling of gas hydrate behavior. Computational Geosciences, 11, No. 2: 117-129.

Kreiter, S., Mörz, T. and Feeser, V., 2007b. Micromechanical control of gas hydrate texture insediment (oral), EGU Joint Assemly. Geophysical Research Abstracts, Vienna, Austria.

Kreiter, S., Mörz, T., Feeser, V. and Grupe, B., in prep. A simulation of gas hydrate growth in marine sediment using the Distinct Element Method - a toolbox for fabric studies. Journal of Structural Geology.

Kvenvolden, K.A., 1988. Methane hydrate -- A major reservoir of carbon in the shallow geosphere? Chemical Geology, 71(1-3): 41-51.

Kvenvolden, K.A. and Lorenson, T.D., 2001. The Global Occurrence of Natural Gas Hydrate. In: C.K. Paull and W.P. Dillon (Editors), Natural Gas Hydrates - Occurrence, Distribution and Detection. Geophysical monograph. American Geophysical Union, Washington, DC, pp. 3-18.

Lee, H., Seo, Y., Seo, Y.-T., Moudrakovski, I.L. and Ripmeester, J.A., 2003. Recovering Methane from Solid Methane Hydrate with Carbon Dioxide. Angewandte Chemie International Edition, 42(41): 5048-5051.

Maslin, M., Owen, M., Day, S. and Long, D., 2004. Linking continental-slope failures and climate change: Testing the clathrate gun hypothesis. Geology, 32(1): 53-56.

McIver, R.D., 1982. Role of Naturally Occurring Gas Hydrates in Sediment Transport. The American Association of Petroleum Geologists Bulletin, 66: 789 - 792.

Mienert, J., Posewang, J. and Lukas, D., 2001. Changes in the Hydrate Stability Zone on the Norwegian Margin and their Consequence for Methane and Carbon Releases Into the Oceanosphere. In: P. Schäfer, W. Ritzrau, M. Schlüter and J. Tiede (Editors), The Northern North Atlantic: A Changing Environment. Springer, Berlin.

Milkov, A.V. and Sassen, R., 2003. Two-dimensional modeling of gas hydrate decomposition in the northwestern Gulf of Mexico; significance to global change assessment. Global and Planetary Change, 36(1-2): 31-46.

Milkov, A.V. and Xu, W., 2005. Comment on "Gas hydrate growth, methane transport, and chloride enrichment at the southern summit of Hydrate Ridge, Cascadia margin off Oregon" by Torres et al. [Earth Planet. Sci. Lett. 226 (2004) 225-241]. Earth and Planetary Science Letters, 239(1-2): 162-167.

Moerz, T. et al., 2003. Deep sourced mounds offshore Costa Rica: A mechanism for non-magmatic forearc recycling of oceanic crust?, EGS-AGU-EUG Joint Assembly. Geophysical Research Abstracts, Nice, France.

Moerz, T. et al., 2005. Styles and productivity of mud diapirism along the middle american margin. Part II: Mound Culebra and Mounds 11 and 12. In: M. G. and B. Panahi (Editors), Mud Vulcanoes, Geodynamics and Seismicity. Nato Science Series. Springer, Baku, Azerbaijan, pp. 49-76.

Moerz, T., Karlik, E.A., Kreiter, S. and Kopf, A., 2007. An experimental setup for fluid venting in unconsolidated sediments: New insights to fluid mechanics and structures. Sedimentary Geology, published online.

Müller, C., Bonnemann, C. and Neben, S., 2007. AVO study of a gas-hydrate deposit, offshore Costa Rica. Geophysical Prospecting, 55(5): 719-735.

Müller, C., Bönnemann, C. and Neben, S., 2002. Detailed Seismic Study of a Gas Hydrate Deposit Offshore Costa Rica (DEGAS). In: A. Rudloff and L. Stroink (Editors), Gas

Hydrates in the Geosystem - Status Seminar. GEOTECHNOLOGIEN Science Report No. 1. Koordinierungsbüro GEOTECHNOLOGIEN, Kiel, Germany, pp. 46-48.
Murariu, V., Svoboda, J. and Sergeant, P., 2004. The modeling of the separation process in a ferrohydrostatic seperator using discrete element method. In: Y. Shimizu, R. Hart and P.A. Cundall (Editors), Numerical Modeling in Micromechanics via Particle Methods - 2004. A. A. Balkema Publishers, Leiden, pp. 119-126.
Paull, C.K. and Matsumoto, R., 2000. Leg 164 overview. In: C.K. Paull et al. (Editors), Proceedings of the Ocean Drilling Program; volume 164; scientific results; gas hydrate sampling on the Blake Ridge and Carolina Rise; covering Leg 164 of the cruises of the drilling vessel JOIDES Resolution, Halifax, Nova Scotia, to Miami, Florida, sites 991-997, 31 October-19 December 1995. Texas A & M University, Ocean Drilling Program., College Station, TX, United States.
Rawn, C.J., 2004. Neutron Scattering 1. Structure and Properies of Materials, Tennessee Advanced Material Laboratory (TAML) Website.
Riestenberg, D., West, O., Lee, S., McCallum, S. and Phelps, T.J., 2003. Sediment surface effects on methane hydrate formation and dissociation. Marine Geology, 198(2): 181-190.
Schmidt, M. et al., 2005. Methane hydrate accumulation in "Mound 11" mud volcano, Costa Rica forearc. Marine Geology, 216(1-2): 83-100.
Shipboard Scientific Party, 1996. Proceedings of the Ocean Drilling Program Volume 164 Initial reports, 164. Texas A&M University, College Station TX.
Singh, S.C., Minshull, T.A. and Spence, G.D., 1993. Velocity structure of a gas hydrate reflector. Science, 260(5105): 204-207.
Sloan, E.D., 1998. Clathrate hydrates of natural gases. Marcel Dekker, Inc., New York, Basel, 705 pp.
Söding, E., Wallmann, K., Suess, E. and Flueh, E. (Editors), 2003. RV-Meteor Cruise Report M54/2+3. Fluids and Subduction Costa Rica 2002, 111. GEOMAR report 111, Kiel.
Spangenberg, E., 2001. Modeling of the influence of gas hydrate content on the electrical properties of porous sediments. Journal of Geophysical Research, 106(B4): 6535-6548.
Stokstad, E., 2003. Ancient Weapon of Mass Destruction: Methane Gas? Science, 310: 1168.
Sultan, N., Cochonat, P., Foucher, J.-P. and Mienert, J., 2004. Effect of gas hydrates melting on seafloor slope instability. Marine Geology
COSTA - Continental Slope Stability, 213(1-4): 379-401.
Sultan, N. et al., 2003. Effect of gas hydrates melting on seafloor slope stability, EGS-AGU-EUG Joint Assembly. Geophysical Research Abstracts, Nice, France.
Thomas, D.J., Zachos, J.C., Bralower, T.J., Thomas, E. and Bohaty, S., 2002. Warming the fuel for the fire; evidence for the thermal dissociation of methane hydrate during the Paleocene-Eocene thermal maximum. Geology (Boulder), 30(12): 1067-1070.
Tohidi, B., Anderson, R., Clennell, M.B., Burgass, R.W. and Biderkab, A.B., 2001. Visual observation of gas-hydrate formation and dissociation in synthetic porous media by means of glass micromodels. Geology (Boulder), 29(9): 867-870.
Torres, M.E. et al., 2004. Gas hydrate growth, methane transport, and chloride enrichment at the southern summit of Hydrate Ridge, Cascadia margin off Oregon. Earth and Planetary Science Letters, 226(1-2): 225-241.
Torres, M.E. et al., 2005. Reply to comment on: "Gas hydrate growth, methane transport and chloride enrichment at the southern summit of Hydrate Ridge, Cascadia Margin off Oregon". Earth and Planetary Science Letters, 239(1-2): 168-175.
v. Stackelberg, M., 1949. Feste Gashydrate. Die Naturwissenschaften, 36(11): 327-333.
v. Stackelberg, M. and Müller, H.R., 1954. Feste Gashydrate II - Struktur und Raumchemie. Zeitschrift für Elektrochemie, 58(1): 25-39.
Villard, P., 1888. Citated in (Sloan, 1998). Compte Redus, 106: 1602.

Webber, B., 2002. The potential of NMR for Gas Hydrate studies, Centre for Gas Hydrate Research, Heriot-Watt University. University of Kent Website.

Yao, M. and Anandarajah, A., 2003. Three-Dimensional Discrete Element Method of Analysis of Clays. Journal of Engineering Mechanics, 129(6): 585-596.

Zatsepina, O.Y. and Buffett, B.A., 1998. Thermodynamic conditions for the stability of gas hydrate in the seafloor. Journal of Geophysical Research, 103(B10): 24127-24139.

Numerical Modeling in Micromechanics via Particle Methods - 2004 - Shimizu, Hart & Cundall (eds.)
© 2004 Taylor & Francis Group, London, ISBN 90 5809 679 3

Numerical simulation of gas hydrate behavior in marine sediments using PFC^{2D}

S. Kreiter
AG. WUM, Technische Universität Berlin, Germany

V. Feeser
Institut für Geowissenschaften, University Kiel, Germany

B. Grupe
AG. WUM, Technische Universität Berlin, Germany

ABSTRACT: The occurrence of gas hydrate at continental margins is considered to be one cause for submarine slope failure and tsunamis in coastal regions. In order to provide the base for a stability prediction of submarine slopes the growth and the decay of gas hydrate was simulated with the two dimensional distinct element method (DEM) of PFC^{2D}. Growing gas hydrate crystals are simulated by a surface tensed ensemble of balls. The influence of surface tension on gas hydrate growth and the influence of gas hydrate growth on the stress state were modeled. Furthermore the decay of gas hydrate located near the sediment surface was simulated. The method used for modeling the surface tensed gas hydrate crystals is supposed to be applicable for the simulation of other polyphase processes, too.

1 INTRODUCTION

1.1 General

Gas hydrate occurring in the sediments of continental margins is a hazard for coastal regions. The decay of gas hydrate was the cause for several submarine slides, some of which created huge tsunamis (Brückmann 2003, Bondevik 2001). This study is part of a joint project with the aim to study continental slope stability. As gas hydrates exist only at high pressure, they are very difficult to sample and to study in nature. It is also very difficult to be handled in soil mechanical experiments in the laboratory, and there the process of gas hydrate growth in fine sediment is very time consuming. Simulations with the distinct element method (DEM) can speed up gas hydrate growth and help to understand the soil mechanical important interactions between sediment and gas hydrate.

Gas hydrate is an ice like solid consisting of water and small gas molecules. Natural gas hydrates contains mainly methane molecules. They form when the constituents come in contact at low temperature and high pressure (Fig. 1). Methane hydrate crystals have the composition 8 CH_4 46 H_2O. They are crystalline solids denser than typical hydrocarbons, so the gas molecules they contain, are effectively compressed. Under normal conditions the melting of methane hydrate releases the 164 fold volume as methane gas and the 0.9 fold volume as water. The volume increase and the high concentration of hydrocarbon in gas hydrates is the cause for soil mechanical impact and for climate effects (Maslin 2004). Furthermore the high hydrocarbon concentration is the base of the potential use of gas hydrate as an energy source (Sloan 2003).

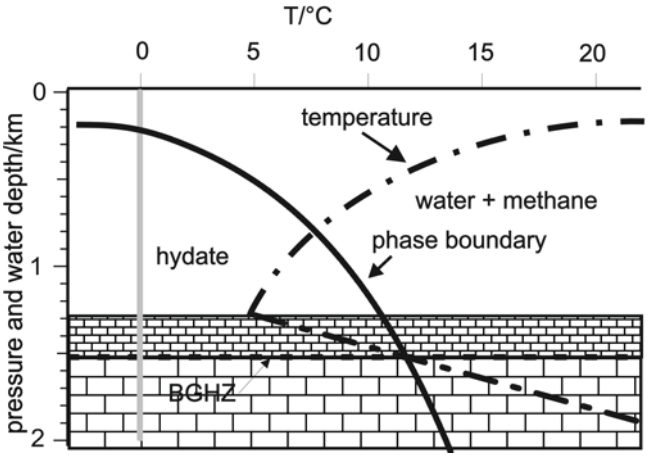

Figure 1. Stability field of gas hydrate and typical temperature pattern in the ocean and the continental slope sediment, BGHZ = Base of Gas Hydrate stability Zone (after Kvenvolden 1987).

The continental margins contain vast quantities of methane hydrates and store more organic carbon than the deposits of oil, gas and coal together (Sloan 1998). They are located in the upper part of

the sediment column in water depths of more than 300 m. In greater sediment depth gas hydrate becomes unstable because of the heat transfer from the earth's interior (Fig. 1). The base of gas hydrate stability zone (BGHZ) is not fixed in room or time, it is highly variable depending on pressure and heat flow. The processes at the BGHZ are until now not well understood, but nevertheless essential for the forecast of submarine slope failure.

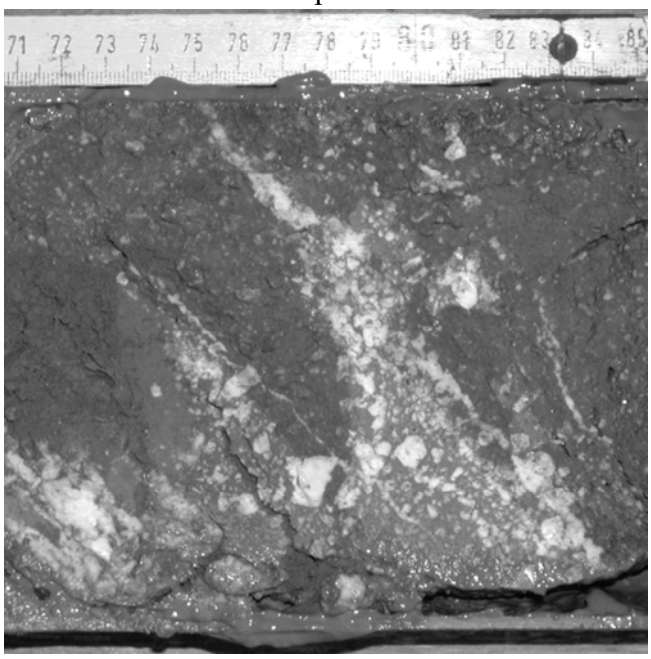

Figure 2. Gas hydrate bearing sediment from the core M54-109, sampled by the R. V. Meteor during the cruise 54 of the SFB 574. (Photo by Tobias Mörz)

Figure 2 shows a sample of gas hydrates in marine sediment. The white lenses within the sediment are gas hydrate. At the time the photograph was taken, the gas hydrate was decaying and transforming the sediment into a mud slurry. This mud slurry is seen at the rim of the core.

Hydrate crystals grow and decompose in the sediment pores depending on changes of the ambient pressure and temperature. These processes change the overall volume in the pore space, and modify the fabric of the grain skeleton. Therefore methane hydrate alters the compaction process and the strength of the sediment. The strength alteration of gas hydrate bearing sediment is important, because the BGHZ (Fig. 1) is found to be the failure plane of several, partly huge submarine slides (Brückmann 2003, Mienert 1998, Mienert 2001).

1.2 Processes related to gas hydrates

In the drilling campaign “leg 164” of the Ocean Drilling Project no gas hydrate was found under a certain sediment depth even though gas hydrate was predicted by the thermodynamic conditions (Rupel 1997). The thermodynamic conditions for the occurrence of gas hydrate were derived from bulk experiments, so the influence of the sediment had to be examined. Natural gas hydrates are growing in the tiny pores of the fine grained sediment and the crystals are therefore forced to form very high curvatures. This led to the assumption that the surface energy reduces the thermodynamic stability of gas hydrates in tiny pores (Clennell 1995, 1999).

Except for coarse sandy sediments all natural gas hydrates found were distributed very heterogeneously in form of lenses or layers (c. f. Fig. 2). So it was postulated that the surface energy of growing gas hydrate crystals in tiny pores is high enough to push the surrounding particles away (Feeser 1997). The importance of the surface tension was confirmed by laboratory experiments which proved that gas hydrate crystals tend to form in the center of the pores (Spangenberg 2001, Tohidi 2001). But the substrate of these experiments being glass beads their results do not apply to the conditions in natural fine grained sediment. Up to now the formation of gas hydrate lenses could not be observed either in soil specimens or in numerical experiments. To asses how gas hydrates grow in the sediment is one aim of this study.

The growth of gas hydrate does not only depend on thermodynamic conditions, but also on the kinetics. The water molecules in the fluid phase are organized in big, relatively stable clusters. These clusters have to undergo severe reorganizations to fit in the crystal lattice of gas hydrates (Sloan 1998).

Under stable conditions of continental margins, steady state upward fluid convection is common. By this convection the fluids are transported deeper and deeper into the stability field of gas hydrate (c. f. Fig. 1) and this could be expected to lead to a homogeneous distribution of gas hydrate in the sediment, but for gas hydrate crystals it is difficult to nucleate. The convection and the hindered kinetics together will cause a slight oversaturation of methane with regard to gas hydrate in the bulk sediment. In contrast once a crystal nucleated will keep on growing, fed by the oversaturated water, depended on the curvature and the surface energy, reducing the oversaturation. The kinetics will then prevent the nucleation of new crystals and is therefore the cause for the inhomogeneous distribution of gas hydrate in the sediment. Very few crystals suffice to create steady state concentration gradients in the continental margin

sediment. So it is reasonable to model the gas hydrate – sediment interaction with the main focus on few crystals and their surface tension.

2 DEM simulation of gas hydrate

The distinct element model (DEM) PFC^{2D} was used as a base for the simulation (Cundall 1978, ITASCA 2002). The gas hydrate related features were added by Fish and C++ routines. The basic idea was to model the growing gas hydrate crystals by growing PFC "balls" and to measure the reaction of the sediment in numerical compression experiments. The simulations in this study were made parallel to the construction of the Gas Hydrate Test System (GTS) laboratory. The GTS is in principle an oedometric compression test but has multiple additional sensors. The numerical experiments performed are adapted to the planned experiments of the GTS.

2.1 Physical concept

The very base of surface tension is the physical interaction between multiple molecules. The behavior of surfaces have been successfully modeled by molecular dynamics simulations (MD). The approach taken here is to simplify the MD models and to scale them up. The up-scaled models then only match the macroscopic behavior of gas hydrates crystals.

The molecular interaction potentials between water molecules and between water and gas molecules are complicated quantum physical phenomenons (Israelachvili 1991), but for practical applications a number of empirical interaction potentials can be used. Because in this simulation only the postulated surface tension has to be simulated, the Mie potential was chosen, which describes the isotropic attraction between hard spheres:

$$w(r)=Ar^{-n}-Br^{-m}$$

where w = potential; r = distance between the midpoints of the spheres: and A and B = adjustable constants. The surface energy of a medium can be calculated by half the energy needed to separate two planar surfaces of this medium. Because the Mie potential is negligible in greater distances, only the nearest neighbors have to be considered. In a dense packing of two dimensional disks (PFC balls) a disk looses two of its six nearest neighbors during the separation of two planar surfaces, so the surface energy γ can be calculated by:

$$\gamma=\frac{1}{2}\left(\frac{2w_{\infty}}{2r_{disk}}\right)$$

with γ = surface energy; w_{∞} = the energy needed to move a neighbor disk from the touching distance to infinity; and 2 r = length of the surface, which is covered by this disk. The energy w_{∞} to move an adjacent disk from the distance σ to infinity in a two dimensions model is calculated by:

$$w_{\infty}=\int_{\sigma}^{\infty} w(r)\,2\pi r dr$$

where w(r) = potential at distance r; σ = the touching distance of the two disk midpoints; and r = actual distance of the two disk midpoints. For different disk radii the constants A and B have to be adjusted in such a way, that the potential minimum of the Mie potential is at the distance in which the disks come in contact. This yields for the chosen exponents n = 3 and m = 6 to:

$$A=\frac{4\gamma\sigma^{2}}{7\pi}$$

$$B=\frac{A\sigma^{3}}{2}$$

with A and B = constants to be adjusted; γ = surface tension; σ = the sum of the two disks radii or in other words the distance between the midpoints of two touching disks. The force originated by the Mie potential is:

$$F(r)=w'(r)=\frac{6B}{r^{7}}-\frac{3A}{r^{4}}$$

where F = force; w = potential; r = actual distance of the disks midpoints; A and B = adjusted constants. This force is only applied when the disks do not overlap. In the case of overlapping disks the standard spring potential of PFC will be used.

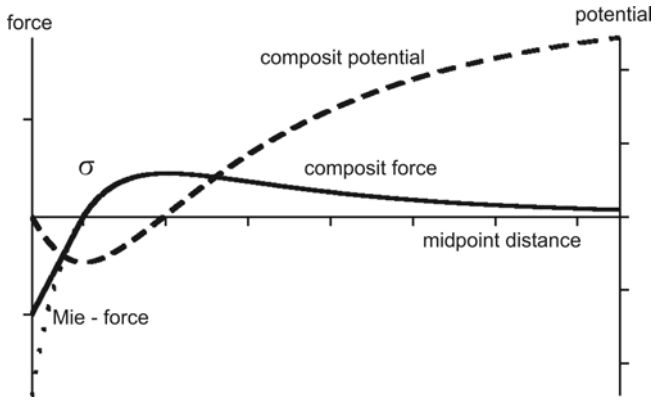

Figure 3. Potential and force over the distance of the two midpoints of the interacting circles (balls), form 10 % overlap to the double of the contact distance.

As shown in Figure 3 the Mie-force and the spring-forces are zero at the distance σ, where the disks touch each other. The potential minimum is at the

same distance.

The growing crystal starts as one disk (PFC ball), but this disk decays if the forces acting on it become too big. The detection of the neighboring disks was performed by the implementation of a PFC "user defined contact law" with a lesser effective radius than the standard contact law. The pictures therefore show no PFC balls but user defined plot objects, the PFC balls are actually strongly overlapping. The overlap makes the neighbor disks accessible by the use of the contact list of the disk (PFC ball).

As the aim of the study was the simulation of gas hydrate growth, the sediment used in the experiments are simple disks with the standard spring contact model and an internal friction.

2.2 Results

2.2.1 Different grain sizes

The virtual oedometric experiment is a box constructed for consolidation experiments, the walls and the bottom of it are fixed, the top can be moved to apply a certain load or to conduct a constant strain experiment. First experiments were made to check the influence of the surface tension on the way gas hydrate crystals grow in the sediment. The nucleation of gas hydrate crystal was implemented by placing a small hydrate disk (PFC ball) into the mid of the pore. The growth of the hydrate crystals was then set to a constant volume per time.

Figure 4 shows the state after gas hydrate growth with the application of surface tension in coarse grained sediment. Figure 5 shows the state after gas hydrate growth with the application of surface tension in fine grained sediment with the same surface tension and the same geometry, but the geometry is five times smaller.

The hydrate crystal in the fine grained sediment stays in round shape and pushes away the surrounding sediment grains. It does not intrude into the edges of the pores. The hydrate crystal in the coarse grained sediment intrudes into the edges of the pores and does not push the sediment grains away until the connected pore space is completely filled up. This clearly illustrates the influence of surface tension when gas hydrate interacts with the sediment grains.

2.2.2 Gas hydrate growth during consolidation

To get a first impression of the influence of gas hydrate on the state and the history of a sediment sample, the interaction of sediment and gas hydrate growth was simulated. The horizontal force was measured to assess the stress conditions in a continental margin sediment in which gas hydrate is growing. The nucleation of the gas hydrate crystals was simulated by a random distribution of several small hydrate balls in the virtual sediment during the preparation procedure, which was done by radius multiplication (ITASCA 2002). The gas hydrate was then growing at a constant rate. In a first experiment the gas hydrate was growing before consolidation and in a second experiment after consolidation (Fig. 6). During the experiment the void ratio, the normal vertical stress and the normal horizontal stress were registered. Figure 7 shows the void ratio over the normal vertical stress. Growing gas hydrate extends the pore space and lets the void ratio rise. Without much vertical stress the rise of void ratio is much higher, and the consolidation starts with a collapse (until Fig.7 point c). Although the history of the samples is quite different, in the void ratio vs effective stress diagram graphs of the two experiments end nearly at the same point.

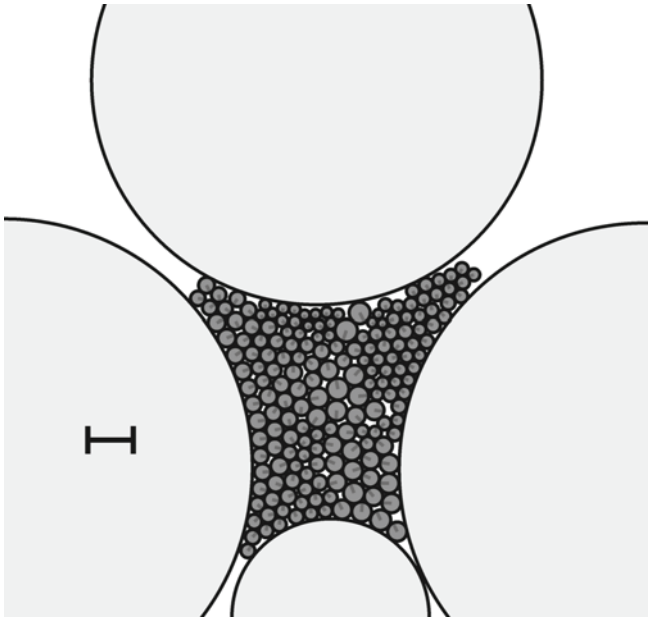

Figure 4. Hydrate growth in coarse grained sediment; dark gray balls are hydrate; light gray balls are sediment. Lines in hydrate balls mark the direction of the applied force. Scale has the same absolute length as in Figure 5.

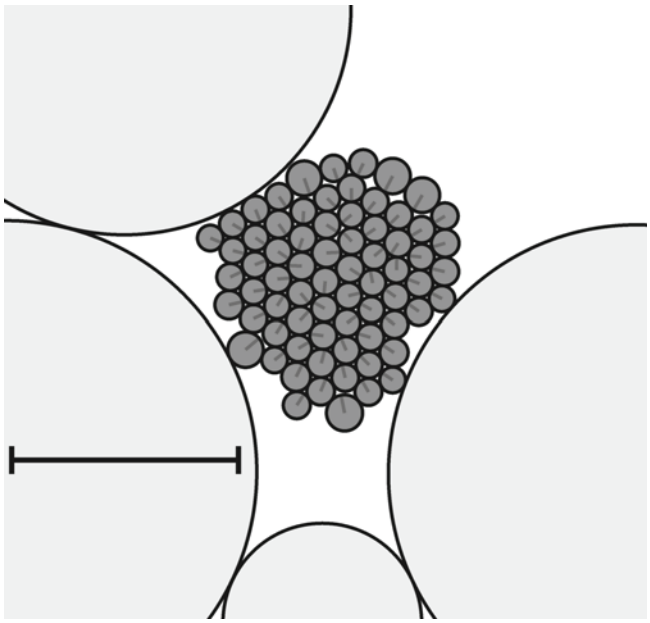

Figure 5. Hydrate growth in fine grained sediment; dark gray disks are hydrate; light gray disks are sediment. Five times smaller than Figure 4, but same relative geometry and same relative hydrate volume as Figure 4. Lines in hydrate disks mark the direction of the applied force. Scale has the same absolute length as in figure 4.

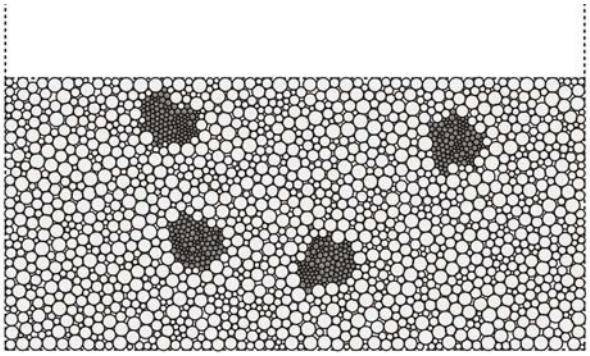

Figure 6. Virtual compression test with gas hydrate, gas hydrate growth after compression. Dark gray balls are gas hydrate; light gray balls are sediment.

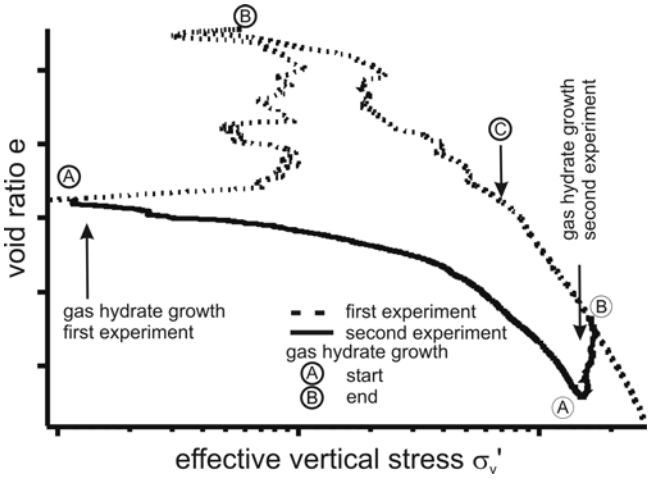

Figure 7. Void ration over vertical stress during gas hydrate growth and consolidation

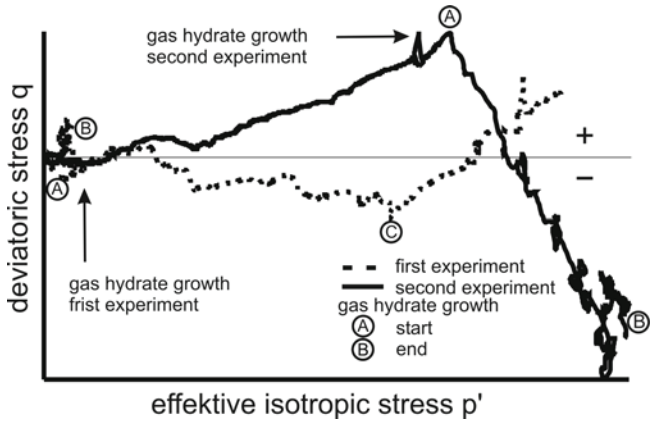

Figure 8. Deviatoric stress over isotropic stress during gas hydrate growth and consolidation

In Figure 8 the deviatoric stress is plotted over the effective isotropic stress. The deviatoric stress which is generated by the consolidation of the first consolidating experiment is reversed by the growth of gas hydrate. In the case of the early growing gas hydrate deviatoric strain can not build up as it would do without a surface tensed crystal in the pore space. The stress state of gas hydrate bearing sediment is shown to be heavily dependent on the history of load application and the history of gas hydrate growth in the sediment.

2.3 Simulation of surface near gas hydrate decay

Most of the gas hydrate research is on surface near gas hydrates, because they are accessible with standard research ships with no possibility to drill and because they are related to interesting structures like mud volcanoes or active faults. In such active environments methane bubbles escape into the free water probably being released from gas hydrate by the warmth of an ascending fluid (Wood 2002). A melting procedure was developed to simulate the surface near decay of gas hydrate to methane. The methane bubble nucleates a random ball of the gas hydrate and growths then in mass balance with the decaying gas hydrate. The methane bubbles were simulated like the gas hydrate crystals as a surface tensed medium out of PFC balls. The surface tension, the mass and the stiffness were adjusted to fit the properties of methane in 1000 m water depth, a depth common for mud volcanoes and other fluid escape structures (Söding 2003). The buoyancy of the methane balls in water is calculated and is applied as an additional force to the methane representing balls. Figure 9 shows the virtual sediment during the process of hydrate decay, Figure 10 shows the resulting methane bubbles in a later stage of the experiment. Some of the methane bubbles are

moving through the sediment, some have escaped in the meantime.

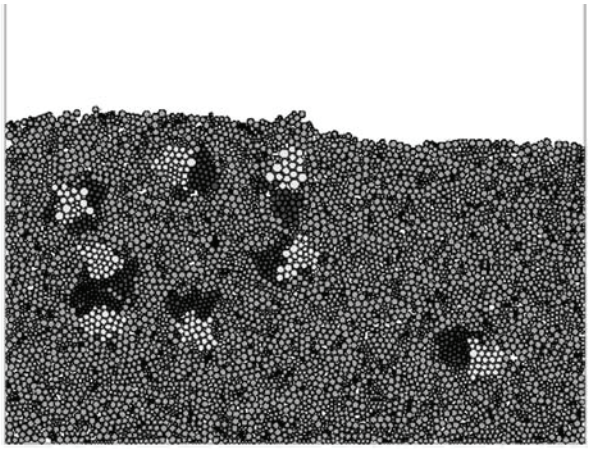

Figure 9. Simulation of gas hydrate decay during the decay. Light gray balls = methane; medium gray balls = sediment; dark gray balls = gas hydrate.

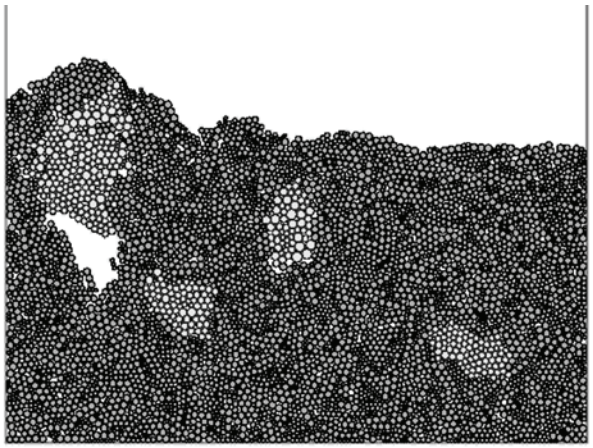

Figure 10. Simulation of surface near gas hydrate decay, after the decay during the escape of the methane. Light gray balls = methane; medium gray balls = sediment.

3 DISCUSSION

Experiments have shown that the simulation of surface tension in the DEM is possible with methods of the molecular dynamic simulation. The influence of gas hydrate growth on the sediment state was modeled as well as the escape of methane bubbles into the water. It is possible to extend the application of surface tensed ball – ensembles to other processes like the freezing of soil or other processes in polyphase mixtures.

The above mentioned oedometric Gas Hydrate Test system (GTS) gives the opportunity to test sediments under the conditions of the BGHZ. This experimental data is needed to validate the way the gas hydrate related processes are simulated. This data will also be used to calibrate the sediment and hydrate crystal properties and to get a deeper understanding of the processes in nature. The calibrated sediment-hydrate ensemble can then be used for other numerical experiments, which measure the shear strength of the sediment like biaxial tests or shear – box tests.

A severe shortcoming of the two dimensional simulation appears during the simulation of gas hydrate growth in coarse grained sediment. The growth of gas hydrate pushes the surrounding particles away because the pore space is not connected. There is no possibility in two dimensions to transfer material to a neighboring pore, so always a sort of overpressure develops and the sediment grains are pushed away. In Figure 4 the uppermost ball is lifted by this process. In three dimensions where the pore space is connected, hydrate crystals would grow around the grains without moving them.

In this state of the model, the pores of the sediment are empty, in real deep sea sediment they are filled with fluids. The presented simulation is therefore only valid for slow changes of stress and at least a medium permeability of the sediment, where the fluid can always escape and no overpressure develops. For faster processes the mechanical influence of the pore fluid has to be taken into account. Also the mass transport within the fluid has not been modeled so far, which is needed to fully understand the formation of the gas hydrate lenses.

4 OUTLOOK

To overcome the known shortcomings of the simulation, it is intended to move to a three dimensional model, with a coupled fluid model and the consideration of mass transport, as detailed the computational costs admit. The properties of the sediment will also be refined to match the properties of a cohesive material.

5 ACKNOWLEDGMENTS

The underlying project was funded by German Federal Ministry for Education and Research (BMBF) under the no. 03G0560A. The authors are solely responsible for the contents of this paper.

REFERENCES

Bondevik, S., C. B. Harbitz, et al. 2001. The Storegga Slide tsunami along the Norwegian coast - from the geological record to numerical simulations (*internet publication*). 2003.

Brückmann, W., C. Müller, et al. 2003. Submarine mass wasting associated with the upper limit of the gas hydrate stability zone at he Costa Rica continental margin. *EGS-AGU-EUG Joint Assembly*, Nice, France.

Clennell, M. B., M. Hovland, et al. 1999. Formation of

natural gas hydrates in marine sediments 1. Conceptual model of gas hydrate growth conditioned by host sediment properties. *Journal of Geophysical Research* 104(B10): 22985-23003.

Clennell, M. B., M. Hovland, et al. 1995. Role of capillary forces, coupled flows and sediment-water depletion in the habit of gas hydrate. *EOS 76* (17, supplement): 164-165.

Cundall, P. A. and O. D. L. Strack 1979. A Discrete Numerical Model for Granular Assemblies. *Géotechnique* 29: 47-65.

Feeser, V. 1997. Gashydratbildung in Tiefseesedimenten - Zur Rolle der sedimentmechanischen Prozess-Steuereung. *DGMK-Tagungsbericht* 9706: 51 - 60.

Israelachvili, J. N. 1991. *Intermolecular and surface forces*. London, Academic Press Limited.

Itasca Consulting Group, I. 2002. PFC2D Particle Flow Code in 2 Dimensions Version 3.0 Manual. Minneapolis, ICG.

Kvenvolden, K. A. 1987. Methane hydrate; a major reservoir of carbon in the shallow geosphere. *Geological Society of America, 1987 annual meeting and exposition*. Geological Society of America. 19; 7: 736.

Maslin, M., M. Owen, et al. 2004. Linking continental-slope failures and climate change: Testing the clathrate gun hypothesis. *Geology* 32(1): 53-56.

Mienert, J., J. Posewang, et al. 2001. Changes in the Hydrate Stability Zone on the Norwegian Margin and their Consequence for Methane and Carbon Releases Into the Oceanosphere. *The Northern North Atlantic: A Changing Environment.* P. Schäfer, W. Ritzrau, M. Schlüter and J. Tiede. Berlin, Springer.

Mienert, J., J. Posewang, et al. 1998. Gas hydrates along the northeastern Atlantic Margin; possible hydrate-bound margin instabilities and possible release of methane. *Gas hydrates; relevance to world margin stability and climate change.* J. P. Henriet and J. Mienert. London, United Kingdom, Geological Society of London. 137: 275-291.

Ruppel, C. 1997. Anomalously cold temperatures observed at the base of the gas hydrate stability zone on the U.S. Atlantic passive margin. *Geology (Boulder)* 25(8): 699-702.

Sloan, E. D. 1998. *Clathrate hydrates of natural gases*. New York, Basel, Marcel Dekker, Inc.

Sloan, E. D. 2003. Fundamental principles and applications of natural gas hydrates. *Nature* 426: 353-359.

Söding, E., K. Wallmann, et al. 2003. *RV-Meteor Cruise Report M54/2+3. Fluids and Subduction Costa Rica 2002.* Kiel, GEOMAR.

Spangenberg, E. (2001). Modeling of the influence of gas hydrate content on the electrical properties of porous sediments. *Journal of Geophysical Research* 106(B4): 6535-6548.

Tohidi, B., R. Anderson, et al. 2001. Visual observation of gas-hydrate formation and dissociation in synthetic porous media by means of glass micromodels. *Geology (Boulder)* 29(9): 867-870.

Wood, W. T., J. F. Gettrust, et al. 2002. Decreased stability of methane hydrates in marine sediments owing to phase-boundary roughness. *Nature* 420: 656-660.

Comput Geosci
DOI 10.1007/s10596-006-9034-6

ORIGINAL PAPER

A distinct element simulation including surface tension – towards the modeling of gas hydrate behavior

S. Kreiter · V. Feeser · M. Kreiter · T. Mörz · B. Grupe

Received: 16 August 2006/ Accepted: 9 November 2006

Abstract Gas hydrate bearing sediments are an integral part of the world's continental margins. Several tsunami-genetic continental slope failure events have been triggered by gas hydrates, but their mechanical behavior is poorly understood. In this work, we propose a method to simulate a surface tensed medium such as gas hydrate in soil, using distinct element method (DEM). For implementation in sediment pore size, we scaled up attractive particle interactions governing surface tension on molecular level. Several virtual experiments are used to benchmark the proposed method. A simulation of gas hydrate growth in sediment with differing grain sizes demonstrates the potential of the new approach.

Keywords distinct element method · gas hydrate growth · grain size effects · PFC · porous sediments · surface tension

S. Kreiter (✉) · T. Mörz
DFG – Research Center Ocean Margins, Bremen University,
P.O. Box 330 440, 28334 Bremen, Germany
e-mail: skreiter@uni-bremen.de

V. Feeser
Institute of Geosciences, Christian-Albrechts-Universität zu Kiel,
Hermann-Rodewald-Straße 9,
24118 Kiel, Germany

M. Kreiter
Max Planck Institute for Polymer Research,
Ackermannweg 10,
55128 Mainz, Germany

S. Kreiter · B. Grupe
AG WUM, Technische Universität Berlin,
Müller-Breslau-Strasse (Schleuseninsel),
10623 Berlin, Germany

1 Introduction

Gas hydrates are a solid high-pressure and low-temperature phase of water and small hydrophobic molecules, and the most common one in nature is methane hydrate ($8CH_4 \cdot 46H_2O$) [1]. Gas hydrates form in the pore space of the continental margin sediment. They frequently occur in all continental slopes in various textures, and there is evidence that they trigger huge continental slope failure events, some of which resulted in destructive tsunamis [2–4]. Gas hydrates are therefore a potential threat to the adjacent coastal regions and all human installations on the slope such as cables, pipelines, and oil platforms. The mechanical properties of such gas hydrate bearing sediments must be known to assess the natural hazards at the ocean margins. Moreover, this knowledge is invaluable in the specific permit procedures and planning of new off shore installations in gas hydrate areas.

The influence of gas hydrate growth and decay in the upper part of the continental slopes sediment on its mechanical behavior was fist discussed by McIver [5] and is the topic of recent research programs such as the construction of GHASTLI and HYDRATECH [6, 7]. A review of gas hydrate related actual research topics was recently given by Beauchamp [8]. Gas hydrate triggered slope failures are also a topic in the climate research community summarized in the "clathrate gun" hypothesis [9], clathrate being a synonym for gas hydrate.

Several mechanical concepts are proposed for gas hydrate growth and decay [5, 10–13]. Most of these concepts are only qualitative and until now there is no unifying model that describes the mechanical properties of gas hydrate bearing sediments. It is generally accepted that gas hydrates do have a substantial influence on the mechanical properties of the sediment; however, the

character and extent of this influence is unclear. Some authors highlight a strengthening of the sediment during gas hydrate growth, due to the consolidation caused by volume reduction and cementation. Other authors emphasize the weakening and disintegration of the sediment during the gas hydrate decay, by water and gas release, volume increase, and reduction of the solid phase.

The textures of the natural gas hydrate observed in sediments testify that their growth in the sediment is a complex mechanical phenomenon. In fine-grained sediment, nodules and layers of different sizes have been found. Since they had been formed after the sedimentation, neighboring sediment was displaced during their growth [14]. In coarse-grained sediments, gas hydrates build a 3D framework cementing them together [15]. However, some fine-grained sediment that formerly contained minor amounts of gas hydrate, as proven by salinity measurements, showed no evidence of relic lenses or nodules [16]. Visual observation and electrical resistivity measurements of model sediment in a high-pressure container show that gas hydrate growth starts in the center of the interstitial sites between sediment grains [17–19]. This implies that gas hydrate is a nonwetting phase relative to sediment grains. The surface energy of nonwetting phases always results in forces in outward direction on the indenting phase. The high curvature in fine-grained sediment may lead to sufficiently high surface forces to push the neighboring grains away, building lenses and layers, whereas in coarse-grained sediments the curvature is low resulting in low surface forces and may allow the gas hydrate to grow around the grains building a rigid 3D network. Thus surface energies may explain the observed textures, and therefore surface tension of the gas hydrate crystal is accepted as a key factor for gas hydrate growth and resulting sediment textures [11, 13]. A quantitative description of this process is still lacking.

Nowadays, computer simulations are an established approach to complement or even partly replace experiments; thus, a reliable simulation of gas hydrate bearing and other sediments behavior would allow funded stability predictions for the continental slope, with only few sediment samples. In this report, we are presenting the first steps towards computer simulation of gas hydrate growth and decay in an arbitrary environment. Our aim is to contribute to the understanding of gas hydrate bearing sediments' mechanical properties and texture.

Although simulation of gas hydrate behavior was the motivation for this study, surface forces are acting at all phase boundaries and are therefore important for many geoscientific questions. Surface forces act on small scales and govern many processes such as crystal nucleation and growth, as investigated in petrology or the microbiological processes covered by biogeochemistry and biogeology. From the geotechnical standpoint, surface tension is known to lead to apparent cohesion of sand in partly saturated soils; furthermore, it affects the permeability for water and the bulk strength [20, 21]. Surface tension in fully saturated soils is, in general, of minor importance because the sand grains do not deform, but if additional phases such as oil or biopolymers are in the system, surface forces on these phase boundaries come into play. Ice and gas hydrate are special cases, because they are solid, but are susceptible to deformations during their growth and during long-term processes. As an introductory conclusion, surface tension in soils is an important issue responsible for many phenomena and applications including the growth and decay of gas hydrate. A new method for the simulation of surface forces may be useful in many geoscientific fields.

2 Concept of the simulation

In the following, the concept of the simulation is developed. It starts with an introduction of the simulation method, followed by the concept used to implement surface tension. We show how the used pair potential is chosen for optimum computational performance. Then, the connection between pair potentials and the surface tension of a two-dimensional discrete material is derived. Finally, some implementation-specific solutions regarding the repulsive part of the potential and variable disk size and cluster growth are explained, before moving on to the benchmark experiments.

2.1 Simulation framework: The distinct element method

The distinct element method (DEM) was chosen as the framework for the simulation, because it focuses on the grain and pore-scale – the scale on which the gas hydrate growth, decay, and interaction with the sediment takes place. DEM models can simulate large displacements and free shear failure planes; in this respect, they exceed the capabilities of classic finite element models. Using DEM, it is not possible to simulate a continental slope in true scale, but enough material can be simulated to measure changes in the bulk properties of the material in virtual experiments. These results can be directly compared to laboratory experiments or used as input for large-scale stability predictions.

DEMs are based on free-moving particles or elements that mutually interact [22]. The movement is governed by Newton's laws of motion. Since the particle interaction is modeled by a continuous potential, they can slightly overlap. Gravity, rigid walls, and other boundary conditions are used to implement a specific model setup. The simulation is fully dynamic in not only leading to a stable

final state, but also in giving the whole development of the simulated process. The problem is solved in discrete time steps, and the minimum length of the time steps in the simulation is determined by the size of the smallest particle and the highest stiffness of the elastic particle interaction. Energy dissipation is provided by a "local" damping where the acceleration arising from collisions is reduced.

DEM is often used together with straightforward physical laws; for instance, magnetic forces were added to the method to simulate an ore separation process [23]. An electrostatic interaction has been implemented in a DEM simulation to optimize the toner transfer in laser printers [24]. Other interactions added were the interparticle forces of clays [25] and apparent cohesion from water menisci between sand grains [26]. The aim of this study was to extend possible interactions in DEM simulations by adding surface tension, a key factor of gas hydrate growth in sediments.

We used the software Particle Flow Code in two dimensions (PFC^{2D}) [27]. PFC is a commercial successor of "Ball" [22]; a description of software-specific implementation issues is given by Kreiter et al. [28]. This study uses a two-dimensional approach, since – for the development of a new method – calculation speed as well as implementation speed are critical.

2.2 Physics of surface tension and the implementation concept

Surface energy is defined as the energy needed to create a new surface (expressed in J/m^2). Surface tension is defined as the force perpendicular to a line on a surface (N/m). N/m can be expanded with m to J/m^2. In the Du Noüy ring experiment [29] described below, this tension force is measured. Although the term tension is mostly used to describe a force caused by the deformation of an elastic medium, thermodynamic surface effects also lead to a tension, referred to as surface tension. Thus, surface tension and surface energy have equivalent dimensions and values, and only semantic differences exist in placing more emphasis on the cause or on the effect of the same processes.

Analysis of surface energy reveals that the attractive interaction between molecules is the cause for surface energy and the related phenomena [30]. Molecules can be treated as particles, and the attraction underlying the surface energy can be directly implemented in DEM simulation. Individual modeling of real-scale molecules leads to very small particles, resulting in very small time steps and far too high computing times. Because of this performance issue, it is not possible to include molecules on their true scale ($\sim 10^{-10}$ m) in a simulation that also contains sand-sized particles ($\sim 10^{-3}$ m) of the sediment. Using up-scaled particles representing hydrate, the attractive interactions have to be scaled to fit the true surface tension. Although much larger than molecules, the hydrate representing particles have to be small compared to the smallest sediment grain.

Cluster size has to be variable to simulate the growth or decay of gas hydrate crystals in an arbitrary environment, and more specific in the pore space of marine sediment. The interaction between this cluster and the environment has to be only dependent on the known surface tension of gas hydrate. The purpose of ensuring this condition is to enable the simulation of virtual gas hydrate bearing sediments, in which texture and stress field development can be analyzed in virtual geotechnical experiments as preliminary shown in [28, 31].

The concept used includes the use of different disk sizes within the gas hydrate representing particle clusters for theoretical and practical reasons. A material composed of disks of the same radius exhibits unwanted pseudo-crystalline properties, resulting in preferential cleavage directions, anisotropic elasticity, and shear strength. In effect, the growing procedure for gas hydrates, which is described below, was designed with the possibility of creating new disks with minimal disturbance while retaining a decent performance. This mechanism involves the use of small and big disks.

2.3 Selection of the used pair potential

The interaction between the particles is given by a pair potential and this potential has to be governed by surface energy. This pair potential has to meet several conditions, such as being zero at infinity and having a minimum value at the particle diameter; however, there are numerous potentials that match those conditions. The length of time steps in the simulation is determined by the size of the smallest particle and the highest stiffness of the elastic particle interaction. Small particles and high stiffness result in small time steps and prohibitively high computing times. The pair potential determines the "stiffness" of the interaction between the gas hydrate representing particles. Another important condition for the physics of surface tension and computational performance is the range of the potential: it should be short [30]. Low stiffness and short range are somewhat contradictory demands for the potential. The last consideration is that the potential should be as simple as possible. The used potential is chosen to match the conditions as best as possible.

In our study, we chose the Mie potential [30] as simple pair potential with one attractive and one repulsive term. It has the form:

$$w(r_d) = -Ar_d^{-n} + Br_d^{-m}. \quad (1)$$

where w is the potential, r_d is the distance between two particle midpoints, and A, B, m, and n are constants with the

condition $n>m$ and $m>3$. In molecular dynamic simulation, a Mie potential with $n=12$ and $m=6$, the Lennard–Jones potential is often used. We examined the key properties of the Mie potential family to choose the best potential for our simulation.

The potential has four independent variables and can be written in the form:

$$w(r_\mathrm{d}) = -Ar_\mathrm{d}^{-n} + Br_\mathrm{d}^{-m} \Leftrightarrow w(r_\mathrm{d}) = A\left(-r_\mathrm{d}^{-n} + \frac{B}{A}r_\mathrm{d}^{-m}\right) \tag{2}$$

The right side of equation (2) shows that parameter A can be regarded as a scaling factor, which is necessary to adjust the strength of the interaction, and parameter B/A is then fixed if a potential minimum is dictated by the particle size, as explained below. That leaves m and n for optimization for low stiffness and short range.

From the potential, a stiffness D_r can be derived in analogy to the spring stiffness D in Hook's law (3) and its underlying potential (4).

$$F = -Dr_\mathrm{d} \tag{3}$$

$$w_\mathrm{Hook}(r_\mathrm{d}) = \frac{1}{2}D(r_\mathrm{d} - \sigma)^2 + w_0, \tag{4}$$

F is the repulsion force, r_d is the displacement, w_Hook is the underlying potential, and σ is the distance (where w_Hook has a minimum value). For a spring, the stiffness is a constant and therefore independent from r_d. For an arbitrary potential w, stiffness $D_\mathrm{r}(r_\mathrm{d})$ is more generally defined as the derivative of the force with respect to the displacement r_d.

$$\mathrm{D}_r(r_\mathrm{d}) = \frac{\mathrm{d}F(r_\mathrm{d})}{\mathrm{d}r_\mathrm{d}} = \frac{\mathrm{d}w(r_\mathrm{d})}{\mathrm{d}r_\mathrm{d}^2} \tag{5}$$

The Mie potential's stiffness increases with decreasing distance. As a typical stiffness value for the comparison of Mie potentials, the equilibrium situation, i.e., the stiffness at the potential minimum, is considered.

The range of the potential is infinite, but the interaction energy decreases rapidly with distance. An effective potential range $r_{\mathrm{d}1/2}$ is defined, where the absolute value of the interaction energy E of one particle with a homogeneous and infinite approximated medium of other particles has decreased to half of its value at the minimum E_min.

$$E\left(r_{\mathrm{d}1/2}\right) = E_\mathrm{min}\frac{1}{2} \tag{6}$$

with

$$E(r_\mathrm{d}) = \int_\sigma^\infty w(r_\mathrm{d})2\pi r_\mathrm{d}\rho\mathrm{d}(r_\mathrm{d}) \tag{7}$$

where ρ is the particle density of this medium and σ is the distance of the energy that reaches its minimum. The integration sums up the interactions for the whole area outside the distance σ to infinity.

As a note to readers who are used to geotechnical notations, we want to stress that the used σ has no connection to the stress notation in geotechnics. The notation σ for the pair potentials minimum distance is adopted from Israelachvili [30], and a very common notation in molecular and surface science was also used by Allen and Tildesley [32].

An analysis of all possible exponent combinations of m and n from 3 up to 12 was performed with A and B adjusted to constant particle size and a constant surface tension, as derived below. The resulting effective distance is plotted versus stiffness at contact in figure 1, with one data point for each Mie potential with exponents n and m. In general, a high exponent m leads to a short range and a high exponent n to an increase in stiffness. As a compromise between low stiffness and short range, the potential has to be as low and left in the diagram as possible. Finally, the potential with $n=6$ and $m=7$ was chosen (figure 1). Another possibility would have been $n=7$ and $m=8$.

2.4 Linking the pair potential to surface tension

Now, the chosen pair potential is linked to the surface energy for the two-dimensional simulation. In two dimensions, surfaces are reduced to contour lines, but in analogy to the physical 3D problem, "surface" is used in this paper for the length of the phase boundary in 2D. Treatment of the potential in three dimensions involves only minor changes.

Although gas hydrate in the simulation consists of arbitrarily placed particles of different sizes, for the derivation of the pair potential the geometry was approximated by a close packing of equally sized disks. The surface energy γ of a material can be calculated as energy E_sep needed to separate two surfaces of the material, normalized by the new created surface area [30]. The interaction potential on the molecular level as well as the upscaled model potential are of very short range; therefore, as a first approximation only the nearest neighbors are considered. Surface energy is deter-

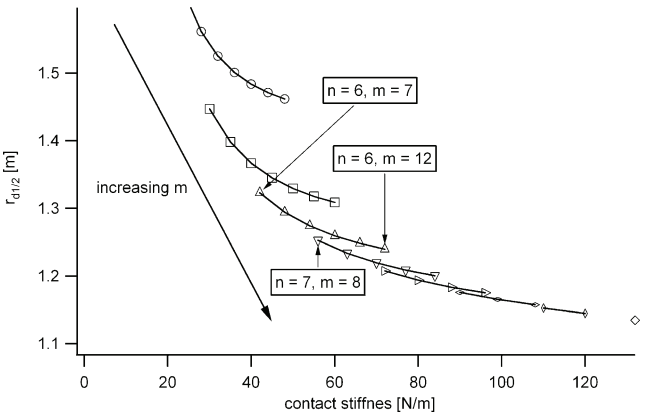

Figure 1 Effective potential range $r_{1/2}$ versus the stiffness at contact for Mie potentials with exponents n and $m<12$. The exponents are indicated for the Lennard–Jones potential and the chosen potential.

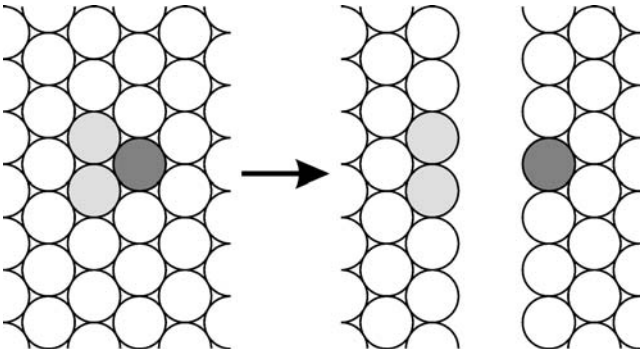

Figure 2 Creating a new surface in a close packed assembly: The dark gray disk and every other disk loses two neighbors, marked in light gray for the case of the dark gray disk.

mined by considering the process sketched in figure 2. A close packed array of disks is separated. During the separation process, each disk loses two of its six nearest neighbors, and two times the disk diameter new surface is created, one on each side of the gap (figure 2).

We define here the disk diameter of two equally sized disks to be the pair potential minimum distance σ. This is just a definition, because particles with an infinite interaction range have no clearly defined size (the average midpoint distance between two neighboring particles in an ensemble is dependent on many factors). The actual movements of the particles modify the midpoint distance over time and space. Although the movements are mainly determined by the pair potential between the nearest neighbors, they are also influenced by interaction with farther neighbors – in terms of overall pressure and excitation from the surrounding material. For short-ranged potentials, not too vigorous excitation and low external pressure the average disk diameter does not differ much from the distance of the minimum of the pair potential, therefore the definition is reasonable. Accepting this allows us to calculate the separation energy E_{sep}:

$$E_{\mathrm{sep}} = 2w(\sigma), \tag{8}$$

where w is the Mie potential (1); the surface energy γ therefore amounts to

$$\gamma = \frac{E_{\mathrm{sep}}}{2\sigma} \tag{9}$$

The potential minimum σ for two particles, with different radii (r_1 and r_2), is defined as

$$\sigma = r_1 + r_2 \tag{10}$$

The potential minimum is where the derivative is zero, and Mie potentials have only one extreme value which is a minimum.

$$\frac{-\mathrm{d}w(\sigma)}{\mathrm{d}\sigma} = 0 \tag{11}$$

The insertion of (8) in (9) leads to the combination in (11), and the exponents n=6 and m=7 in (1) and rearranging yields the following equations for A and B.

$$A = 7\gamma\sigma^7 \tag{12}$$

$$B = \frac{6A\sigma}{7} \tag{13}$$

The attractive force is calculated by:

$$F(r_{\mathrm{d}}) = \frac{\mathrm{d}w(r_{\mathrm{d}})}{\mathrm{d}r_{\mathrm{d}}} = -\frac{6A}{r_{\mathrm{d}}^7} + \frac{7B}{r_{\mathrm{d}}^8} \tag{14}$$

where r_{d} is the distance between the centers of the disks and F is the force between the disks.

2.5 Implementation-specific issues

The simulation is designed for differing and dynamically changing disk sizes (10), so A and B are calculated at each time step for every pair. The potential is only applied for separated disks (i.e., $r_{\mathrm{d}}>\sigma$). For interpenetrating disks the repulsive force is derived from a standard spring type potential (4) provided by the software package. The use of spring type potential allows users to define a maximum stiffness and so the simulation can benefit from the automatic time step detection of the software package, which is based on the theory of multiple mass spring systems [27]. A simulation with a theoretically infinite stiffness would necessitate the implementation of another time step detection scheme, with the risk of adding overhead and producing erroneous or unstable results. The interpenetrating stiffness was first set to the stiffness at contact, but that produced large interpenetration of the disks. Several simulation runs revealed that a stiffness of four times the Mie stiffness at contact results in satisfactorily low interpenetration and reasonably long time steps. The resulting force and potential are shown in figure 3, and the stiffness in figure 4.

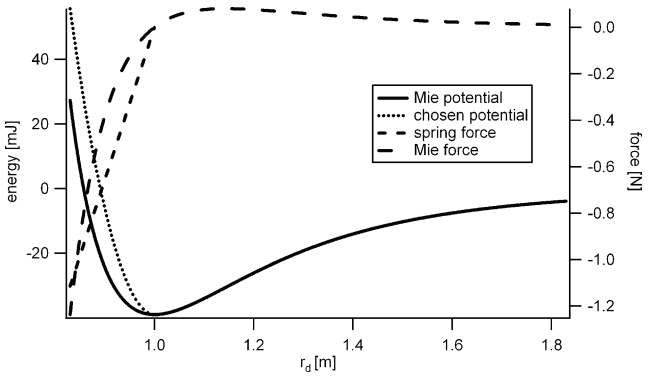

Figure 3 Distance dependence of the Mie potential with the exponents n=7 and m=6, and the resulting forces for two disks with a diameter of 1 m and the surface tension of 0.039 J/m^2.

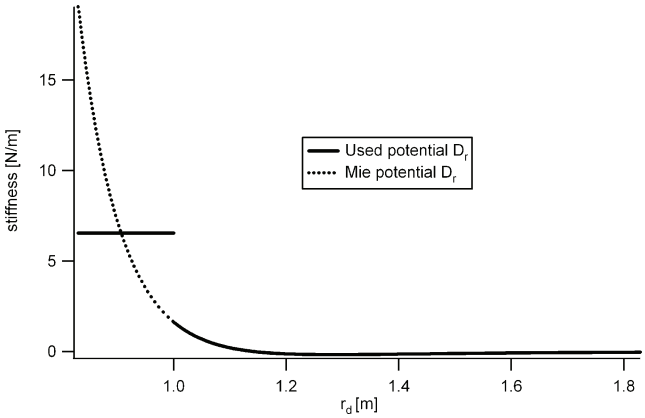

Figure 4 Distance dependence of the stiffness of the chosen and the Mie potential of figure 3.

The chosen potential has a discontinuity in the stiffness, but that causes no problem during the simulation because the underlying force is continuous, and this is the term (value) used in the simulation. The underlying potential is actually differentiable.

For large particle ensembles, calculation of the interaction between every pair intolerably degrades the performance of the calculation; therefore, the possibility to cut off the potential at a certain distance was included in the code and the cutoff distance is chosen after the experiments described below.

Growth of the gas hydrate is simulated by two mechanisms: (1) the gas hydrate representing disks expand; (2) disks exceeding a maximum radius are substituted by three small disks (figure 5a). The large and small disks are termed child and parent, respectively. This maximum radius is defined as a fraction of the minimum radius of the surrounding nonhydrate disks; in this work, this fraction was set to 1/30th. The new "child" disks fall completely inside the circle defining the parent disk to avoid the forces that would result from overlap with their neighbors. This procedure reduces the overall area of the disks; this reduction is compensated by the fast growth of child disks during the following calculation steps.

The decay in three disks is a compromise between minimum area loss and maximum resulting child radius (figure 5b). The main breaks in the area fill ratio curve is from two to three and from six to seven children, whereas the child radius shrinks nearly linearly form two to six children. Therefore, three child disks were taken as a best option.

To avoid shock wave formation resulting form fast particle growth, the radius expansion in one time step, Δr, has to meet two conditions: First, the energy introduced by the possible overlap generated by the expansion of the radius is set to a fractional amount *fract* of the separation energy. The overlap energy is calculated after (4), whereas r_d–σ is replaced by Δr_E. A factor of 2 is introduced to account for the possibility of two expanding disks in contact. Separation energy E_{sep} is obtained by inserting (1) in (8).

$$\left(-A\sigma^{-6}+B\sigma^{-7}\right)\mathrm{fract}=\frac{1}{2}D(2\Delta r_E)^2 \tag{15}$$

yielding

$$\Delta r_E=\frac{\sqrt{\mathrm{fract}\left(-A+\frac{B}{\sigma}\right)}}{\sqrt{2D\sigma^3}}. \tag{16}$$

Note that the disks expand; therefore, Δr is positive. Second, the radius expansion must be smaller than the distance that this particle moves in one time step Δt. This distance, Δr_t, is approximated by using (3), Δr_E from (16), and the force–acceleration law by

$$\Delta r_t=\frac{D\Delta r_E\Delta t^2}{2\pi\left(\frac{\sigma}{2}\right)^2\rho}. \tag{17}$$

When performing the disk's radius expansion, we use either Δr_E and Δr_t for whichever is the lower value in each case. A fractional amount of 0.2 was used for the calculations of (16) in this paper.

The growth mechanism was only used for the simulation of gas hydrate growth in the sediment. Gas hydrate decay can be simulated by shrinking and deleting of single gas hydrate disks.

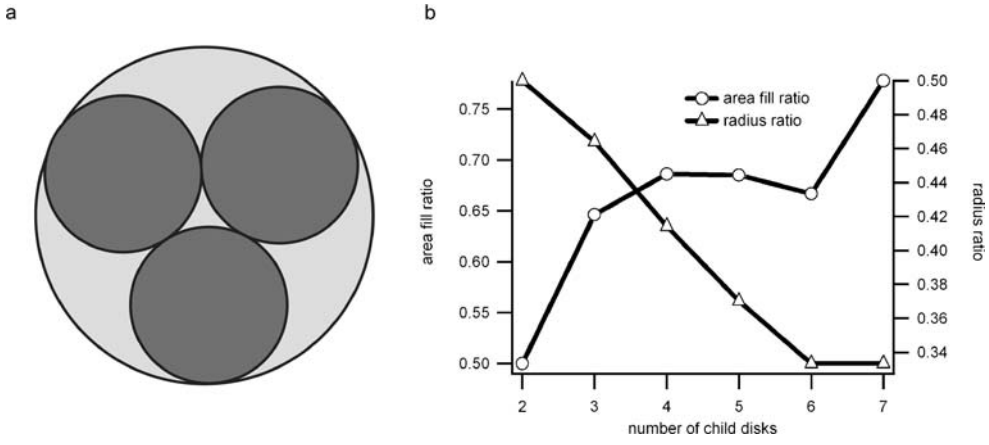

Figure 5 (a) Geometry of the disk splitting process. Parent disk and child are shaded in light and dark gray, respectively. (b) Key parameters that guided the choice of child to parent geometry during the splitting and replacement process. Area fill ratio: area of parent disk minus sum child disks area normalized by the parent disk area. Radius ratio: child disk radius divided by parent disk radius.

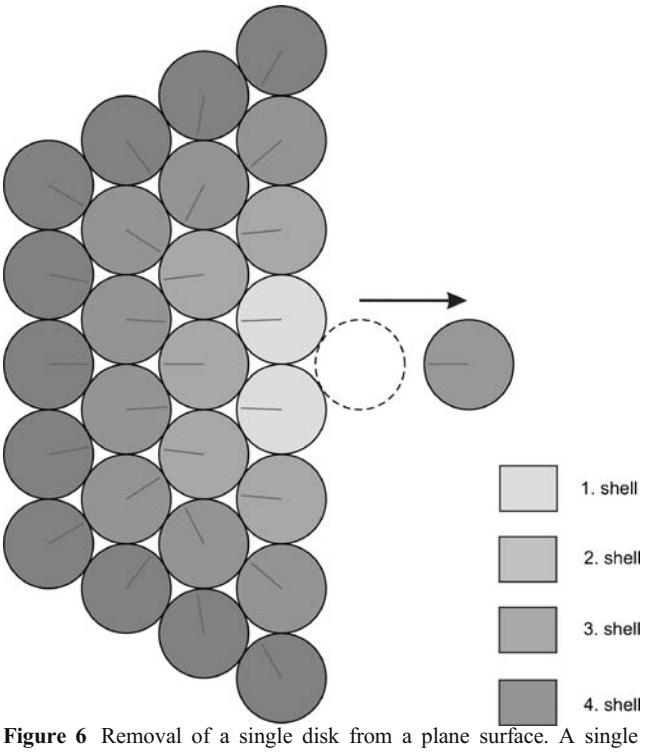

Figure 6 Removal of a single disk from a plane surface. A single probe disk moves to the right, the initial position is shown in dashed lines, the different shells of the close packed disk ensemble are indicated by gray shades. The direction of forces acting on the disks is indicated by dark lines starting in the center of disks.

3 Experiments

The theoretically derived potential was benchmarked by simulations described in the following section. The experiments start with close packed ensembles, proceed to random ensembles, incorporate free movement, and finally simulate the growth of gas hydrate in a sediment pore.

3.1 Close packed ensembles

The first experiment was designed for two purposes: (1) to test the general usability of the simulation code and (2) to investigate the influence of disks more than a diameter away in a regular, but reasonable geometry scenario. For this purpose, the energy needed to detach one disk from a close packed ensemble of equally sized disks was analytically calculated and simulated. One probe disk is placed in contact to an ensemble of close packed disks. An experiment with four "shells" is shown in figure 5. Simulations were performed for analogous geometries with 1, 2 to 10 shells. The pairwise attractive interaction derived above (14) is applied to all disks. No free movement is permitted, the position of the close packed disks is fixed, and the probe disk is moved apart in a predefined number of time steps to a distance of 10 times the diameter of one disk. The energy E required to overcome the attractive force is recorded during the experiment by reading out the force and the displacement r_d for each calculation step:

$$E \sum_{\text{steps}} \vec{F}\,\vec{r}_d \tag{18}$$

To illustrate the internal interactions, the direction of the resulting attraction is shown for each disk.

Figure 7 shows the resulting energies of the virtual experiments and the analytical solution of the equivalent problems using equation (1) and the known geometry relations of the close packing. In contrast to the simulation, where the separation stops at a distance r_d of 10 times the disk diameter, the analytical calculation is solved for infinite separation.

Constants A and B are calculated after (12) and (13) to match a surface energy of 1 J/m. The diameter of the disks is 0.5 m, thus the separation energy of the two nearest-neighbor disks is expected to be 1 J (8). The simulation with one shell is equivalent to the geometry used for the derivation (compare figures 2 and 6). In this case, the simulation with 2000 steps yields 1 J and therefore correctly reproduces the derivation geometry.

Calculations with more layers show that the outer shells increase the separation energy to 132.9% of the value obtained when considering next-neighbor interactions only. The difference corresponds to approximations used during the derivation. It confirms that most of the energy arises from the interaction with the nearest neighbors, but also that a minor and nonnegligible amount of energy is contributed by the farther surrounding. However, the contribution of layers beyond layer 4 is negligible, reflected in constant values of the separation energy of layer 4 or greater (figure 7).

Since naturalistic models always include numerous particles, resulting in large number of layers, a correction is needed. For the case of multiple close packed disks, the multiplication of the input surface tension with 1/1.329 gives

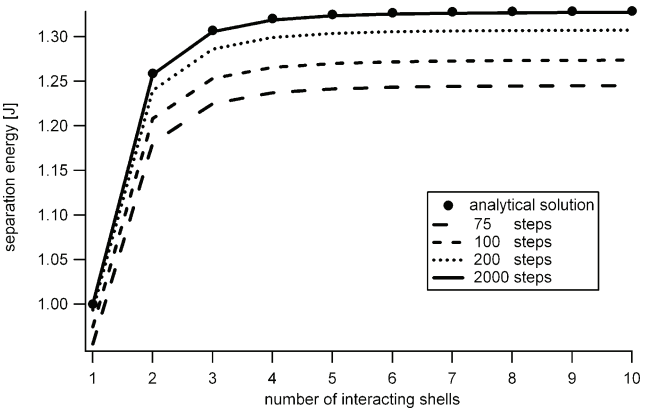

Figure 7 Diagram of the separation energy plotted versus the number of shells of a close disk packing interacting with the probe disk (q.v. figure 6). Filled circles show the energy derived from the analytical solution; lines show the results of DEM simulation using different numbers of steps.

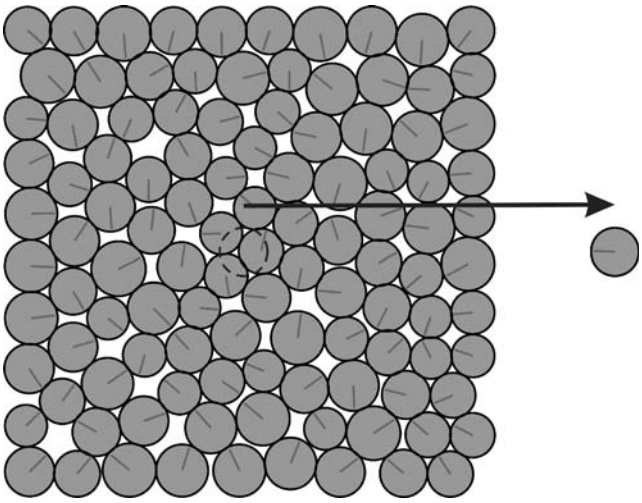

Figure 8 Snapshot of a virtual experiment involving 110 randomly assembled disks with a ratio of 1.3 between the largest and the smallest disk. The probe disk is moved out of the square disk ensemble, and its starting location is indicated by the dashed contour; the arrow shows the movement of the disk. The direction of attractive forces acting on disks are indicated by the dark lines starting in the center of the disks.

the desired result. Particle arrangements that differ from close packing (e.g., as in figure 8) require other correction factors.

Furthermore, it can be noted that the simulation reproduces the analytically calculated energies as perfect as desired if enough time steps are run. The error introduced by coarse time step resolution adds in this case up to a maximum of about 10%.

3.2 Random ensembles

The next experiment was carried out to evaluate the influence of complex disk arrangements, which cannot be treated with simple analytical calculations. It was designed to check how a randomly assembled disk packing and different disk sizes influence separation energy. Another question was, how many disks are required in an ensemble of disks to obtain constant separation energy? The fixed, artificial boundary conditions, where only one disk is allowed to move in a given mode, were retained for reasons of simulation efficiency and to exclude the influence of particle movements.

A disk is moved out of a square of randomly assembled disks with varying particle diameters (figure 7). A block of disks with a random radius distribution was generated via the standard radius multiplication procedure of PFC^{2D} [27]; subsequently, the positions of the disks are fixed. A probe disk is generated in the center of the block, and moved outward, while recording the energy of the attractive forces. Repulsion forces due to overlaps are not recorded.

The energy required to move the probe disk against the attractive forces is calculated using equation (18) (figure 9). The resulting energy is given as a function of the probe position in figure 8. Inside the particle ensemble, the energy oscillates around zero, and after the probe reaches the edge of the ensemble the potential rises rapidly to a constant level. Fluctuations inside the block depend on the geometry; therefore, different starting geometries have slightly varying energy levels. This potential of several disks with random relative positions can be compared to the smooth potential of two disks in figure 3.

The extraction energy of the disk was then normalized to the equivalent new surface produced to obtain a value that can be compared with the surface energy. The surface was calculated according to equations (8) and (9) by assuming that an average of six neighbors has been lost (see figure 2). Looking at the derivation, where two close packed materials are separated, this is equivalent to a surface of six times the diameter of the disk (figure 2). The result of a series with different numbers of disks is shown in figure 10.

It can be seen that ensembles of 10–20 disks and more exhibit constant normalized extraction energy, so an ensemble should at least contain 10 disks. The observed maximum extraction energy is higher than the energy derived from a nearest-neighbor interaction because of the

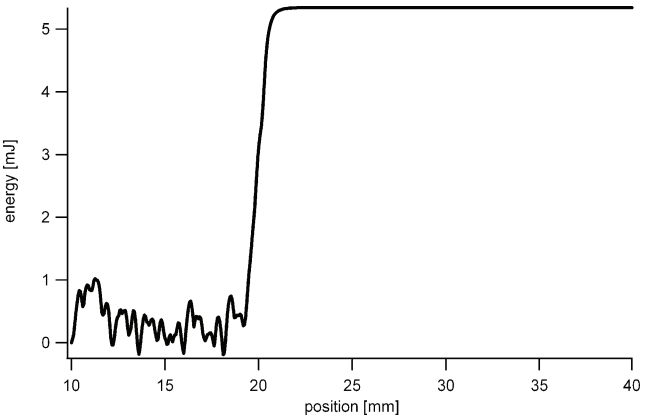

Figure 9 Energy needed to move the probe disk against the attractive potential. Box size 20 mm, middle of the box is at 10 mm.

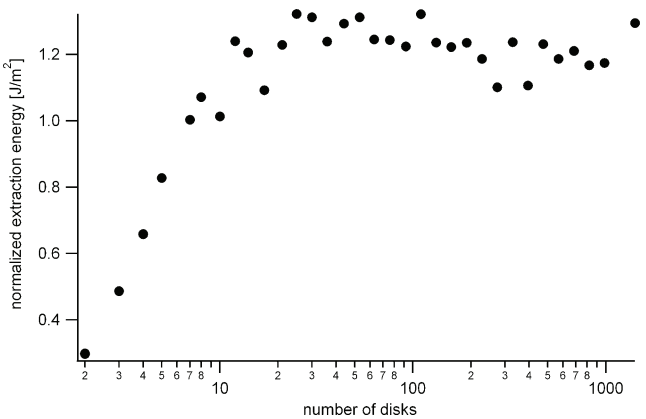

Figure 10 Normalized extraction energy vs. number of disks in the square disk ensemble. Note the log scale on *x*-axis.

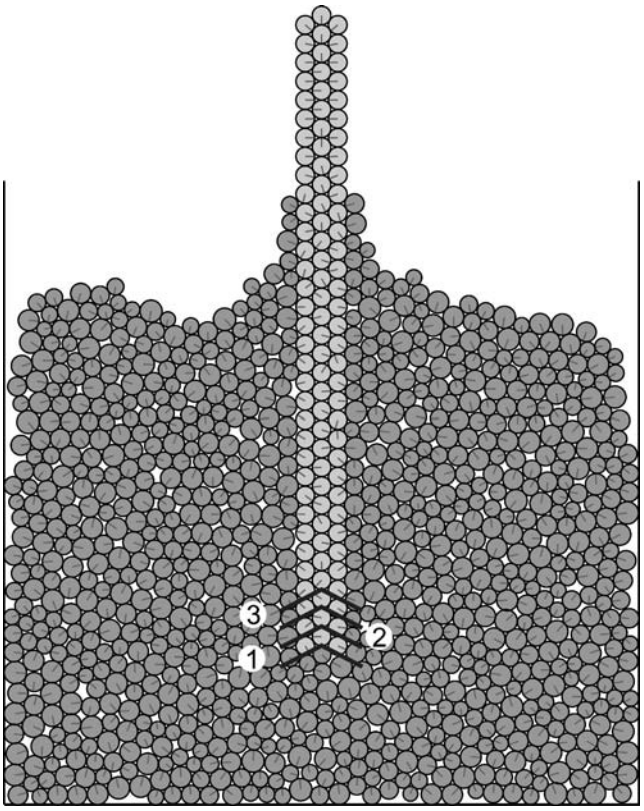

Figure 11 Setup of the virtual Du Noüy ring experiment with 1000 disks. The fluid film is represented by the block of light gray dense packed disk in the middle of the experiment. Dark gray lines starting in the center of the disks indicate the direction of forces acting on the disks. Note the climbed meniscus around the "fluid film" and the convex shape near the noninteracting walls. The average kinetic energy was lowered in order to obtain a well-defined free minimum energy surface. In the lower part of the rigid probe, the distribution of disks in horizontal layers is illustrated.

long-range influence of the potential, as already observed in the previous section, although lower than that in the close packed case (figure 7). The packing appears looser because the lacking particle movement results in large overlaps, which are equivalent to void space for this special setup. The long-range interaction and packing correction factor is, in this case, approximately 1/1.2.

The cutoff distance of the potential was examined via a similar series of experiments leading to a distance at least 3 times the particle diameter for acceptable results and 6 times for quasi-perfect matching with a non-cutoff potential; the latter was chosen for the following simulations.

The influence of the size of the probe was explored during another experimental series. A smaller-than-average probing disk results in larger observed extraction energy, and a larger-than-average probe disk diameter results in smaller observed extraction energies. Further experiments were carried out to test the influence of the ratio of the largest to smallest disk radius while using the average radius for the probe. These experiments show that only the scatter of the measurement changes. To summarize, we state that the use of different disk sizes introduces artifacts if we focus only on single disks, and that these artifacts average out when the whole ensemble is considered.

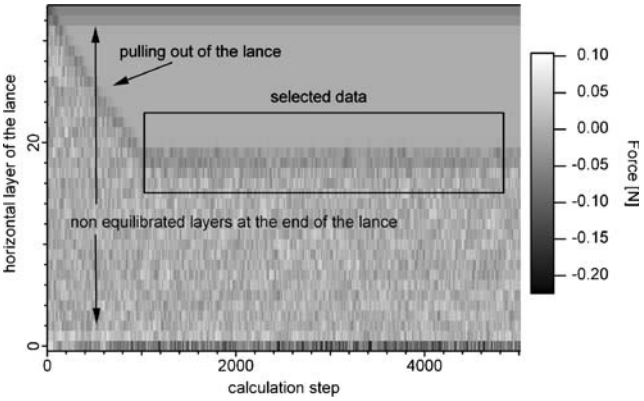

Figure 12 Plot of attractive forces on each horizontal layer of the probe as gray shades – the darker the color, the higher the force in downward direction. The framed area corresponds to layers and time steps taken for further evaluation. In the first 1000 steps, the probe is moved upward, out of the particle ensemble.

3.3 Du Noüy ring experiment – free moving ensemble

Bearing in mind that the simulations should reproduce realistic experimental conditions, a virtual equivalent of the du Noüy ring experiment [29] was developed. In this experiment, the surface energy is determined by measuring the maximum force the fluid exerts on a film that is held by a ring until the fluid film ruptures. The fluid is simulated by a box full of freely moving disks (figure 11). As equivalent of the fluid film, a rigid probe of close packed disks is used, and medium-size disks of the probe were used to avoid sampling bias that arises from using varying disk sizes. The attractive interaction is applied between all disks and the correction factor of 1/1.25 was used.

Several failed experiments have shown that an adjusted attractive potential alone does not suffice to simulate a surface tensed fluid with a particle method. The inter-

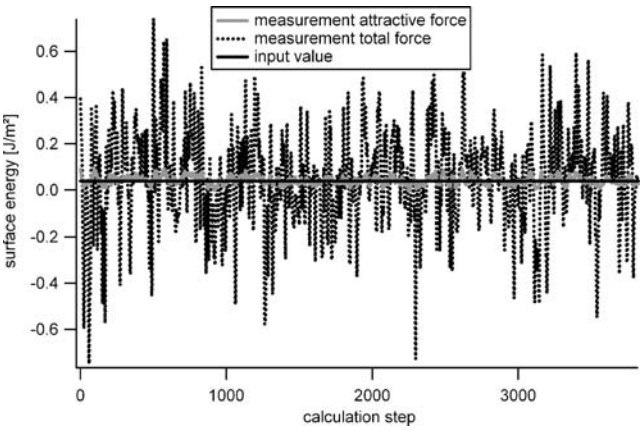

Figure 13 Surface energy calculated from the attractive force and total force measurements.

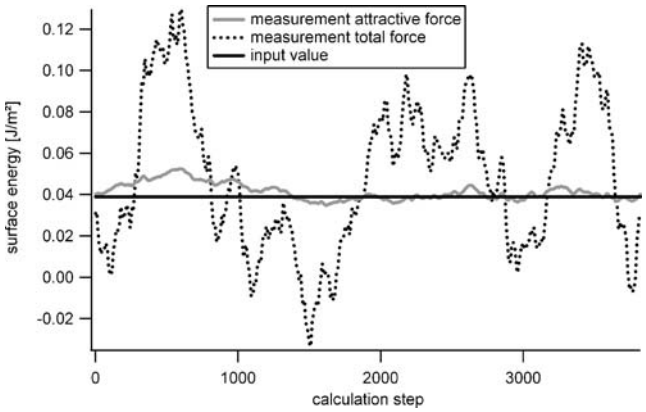

Figure 14 Moving average of 500 values of the surface energy calculated from the attractive force and total force measurements.

locking of particles inhibits the formation of minimum energy surfaces, and the material exhibits a brittle type of failure and is in a sort of solid state. Neither the resulting geometries nor the surface energy measured by the du Noüy method is realistic. Our solution was to "melt" the material to the fluid state. As the underlying principle of temperature is the average kinetic energy of molecules, we added random particle movements to the disk ensembles. A random number generator is used to create velocity vectors with random directions that are, in turn, assigned to the disks until the desired average kinetic energy level is reached. Slight damping is applied to dissipate the energy added by other means to the system. The slight energy dissipation is balanced by adding a few new random movements and the average kinetic energy is held constant. As a result, the material deforms in a nonbrittle way and forms minimum energy surfaces.

The average kinetic energy can not be related to meaningful Kelvin temperature, because the simulation is scaled up and the moving particles have differing masses. The average kinetic energy needed to attain a fluid state is expected to vary with the disk size.

Simulation of the fluid film by close packed disks is a simplification, which has to be kept in mind for the analysis of experimental results, and implies several consequences.

First, the ends of a probe built by a close packed ensemble are not in equilibrium, because of the long-range interaction of the disks. Although the nearest neighbors to the disk at the end of the probe are in contact and therefore exert no forces, the farther neighbors attract the probe in an inward direction and cause nonequilibrium forces. These nonequilibrium forces have shown to be in the range of forces to be measured and can not be neglected. They can be seen from the directions of the forces of the top of the probe in figure 11, and from the upper and lower margins of the gray shade plot in figure 12. In the middle part of the probe, the disks are free from this artifact and therefore this part is used for further analysis.

Second, the density of the close packed ensemble is in general not the same as the density of the surrounding bulk material particle ensemble, and the disks forming the probe are not in random movement. This leads to vertical buoyancy forces originating from the sum of the collisions, which have been found to sum up to a significant artifact for long probes.

To reduce this artifact, the part of the probe used for the measurement has to be as short as possible, but has (nevertheless) to include all surface effects. Therefore, a gray shade plot is generated to visualize the force development of the probe in space and time (figure 12). The probe is divided into layers as drafted in figure 11, where every area in the plot corresponds to a defined time step and a defined layer of the probe. The plot is divided in two areas: one showing the same shade and another with fast-changing gray shades. The first area corresponds to times and vertical sections of the probe where there is no interaction with the free-moving disks; the second corresponds to times and sections where the changing positions of the disks lead to quickly changing forces and shading. The top and the bottom borders of the figure correspond to the ends of the probe, and the differently shaded bands there are caused by the end artifacts described above. In the beginning of the experiment, the probe is fully immersed in the box containing the free-moving disks and is then pulled out, which can be observed by the triangular shape of the evenly shaded part from the left to the right. The zone

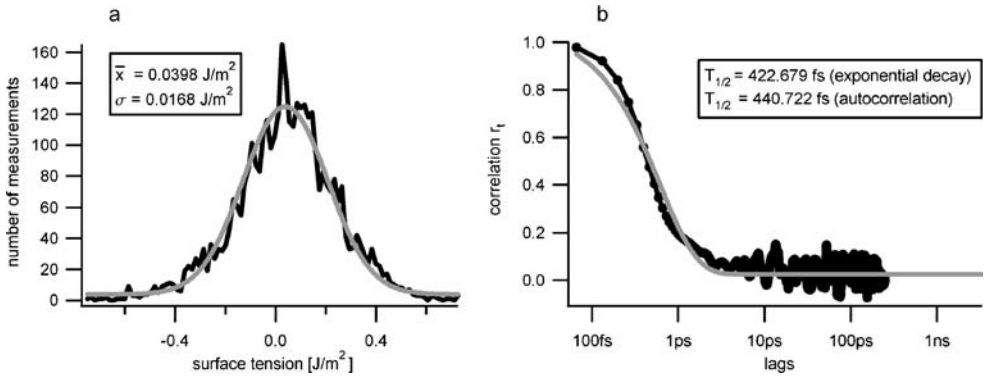

Figure 15 (a) Frequency distribution of data shown in figure 13. The gray line is a fit of the data to a normal distribution mean x value and standard derivation are shown in the inset. (b) Autocorrelation of the same data. An exponential decay (gray line) is fitted to the data. $T_{1/2}$ indicates the half-life of the correlation.

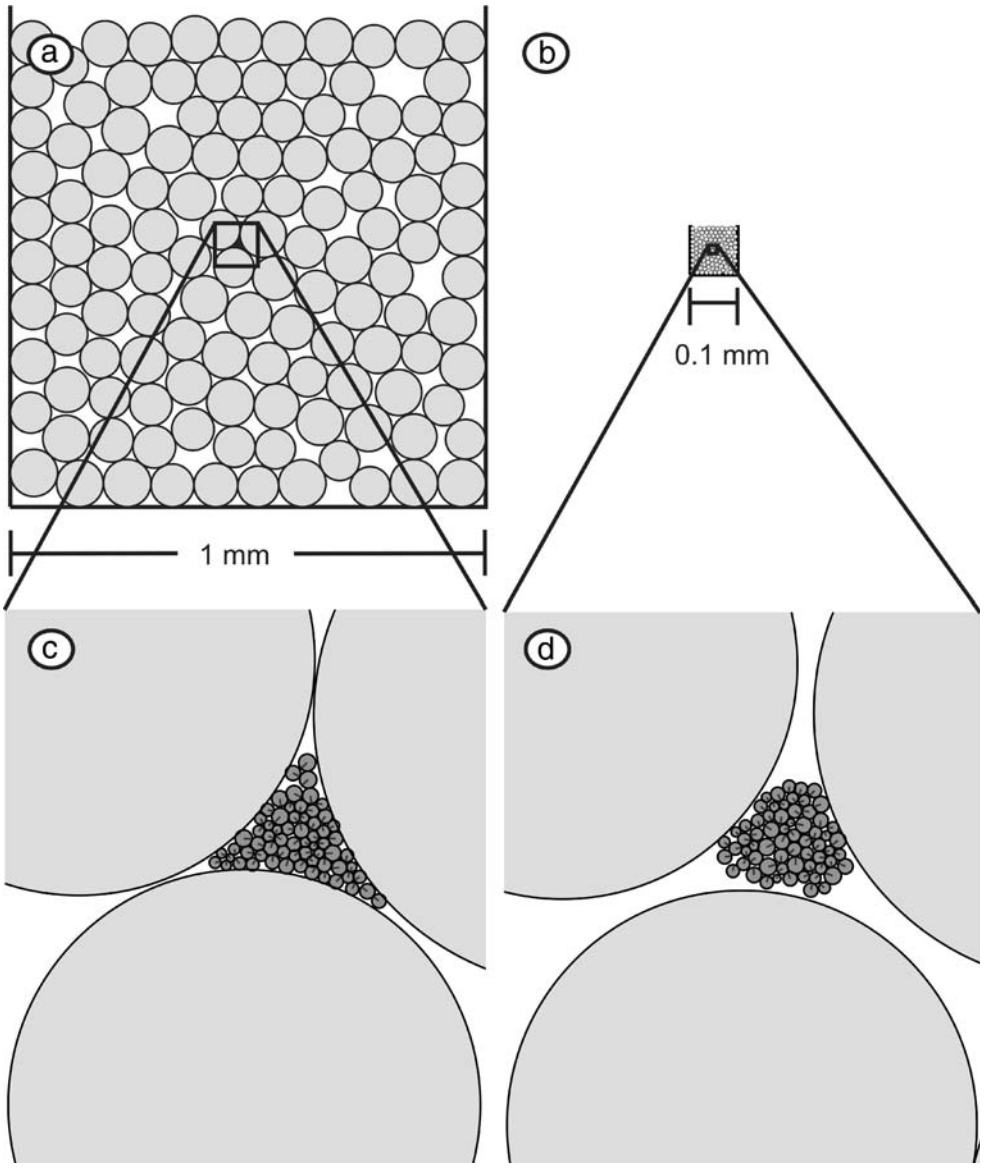

Figure 16 Geometry after gas hydrate growth in two virtual sediment samples with differing grain size. (a and b) Configuration of the sand (~0.091 mm diameter) and silt (~0.0091 mm diameter) grain size experiments, respectively. (a) and (b) are shown on the same scale, indicated by the scale bars. (c and d) Details of the gas hydrate in the sand and silt pore space.

influenced by the surface forces can be seen from darker shading near the interface of the two main areas. The vertical probe section and time period used for further analysis in the experiment is shown as a rectangle.

The measured surface energy of the experiment is shown in figure 13. The total force and attractive forces measured, and the surface energy is derived for each of them by

$$\gamma = \frac{F}{2} \tag{19}$$

In figure 14, the moving average of the same data is shown. The measurements oscillate around the value that was used as input value for the simulation to calculate the particle interaction. This proves the applicability of the method to free moving ensembles and especially for the simulation of gas hydrate growth in confined pore space.

The probability distribution of the extracted surface energies shows a normal distribution, and the mean value matches the simulated surface tension of 0.039 J/m^2 (figure 15a). The autocorrelation shows that the measurements have a red noise overprint. The correlation decay cannot be exactly fitted with an exponential decay law, but nevertheless shows a similar behavior. From the autocorrelation, a typical half-life period ($T_{1/2}$) of 440 fs is recorded, which corresponds to about seven calculation steps (figure 15b). This period must be simulated at least several times, until the systems' reaction to an applied disturbance can be expected or a statistically independent value can be obtained.

3.4 Gas hydrate growth in the pore space

The last virtual experiment simulates gas hydrate growth in the pores of sediments with different grain sizes. It is more

a proof on concept that a thorough analysis of gas hydrate growth in the sediment is currently pursued and will be the subject of a further study. Simulation of the sediment grains is kept simple by using rigid round grains with a stiffness of 3.8×10^{10} Pa and a friction of 0.3, simulating quartz-dominated sediment with medium rounded grains. The gas hydrates surface tension is 0.039 J/m^2 [33]. We used 0.078 J/m^2 for our two-dimensional simulation, because the interface pressure for a given radius of a sphere is double the interface pressure of a cylinder. A tiny disk acting as seed for gas hydrate crystal growth was added in the pore space and additionally to the pair potential; the growth mechanism was used.

A sand- and a silt-sized specimen were prepared, both having the same relative initial geometry. The amount of gas hydrate that has grown was scaled with grain size, and the geometry after gas hydrate growth in the pore is shown in figure 16.

In fine-grained sediment (figure 16d), the gas hydrates surface force is pushing the neighboring grains away; in the coarse grained sediments (figure 16c), the pore space is completely filled. This is in good agreement with observations in nature, as discussed in the Section 1.

Although we think that our method is valid for simulation of gas hydrate texture, there are problems with the 2D approach that cannot be overcome. There is no way to transfer gas hydrate disks from one sediment pore in the neighboring pore without moving the sediment grains; in other words, the pore space in 2D is not connected. As a consequence, the simulation of a 3D sediment cementing network is impossible and the simulation of vast amounts of gas hydrate in coarse sediment in 2D should be regarded with caution.

4 Summary

Attractive forces for simulating surface tension using an ensemble of distinct elements are derived for arbitrary disk geometries and scales, and are tested in a series of experiments.

The experiment with hexagonal close packing revealed that (1) simulation reproduces the geometry used for the derivation perfectly, and (2) a slight long-range influence and packing correction is necessary to correct the surface energy. The need for a slight correction is consequently observed in all other experiments.

Simulation of random packing revealed four important results: (1) The method is applicable to random packing. (2) The minimum number of disks for a cluster with bulk properties is about 10. (3) Use of differently sized disks introduces artifacts when focusing on one disk, but these artifacts average out when regarding a whole cluster with a balanced disk size distribution. (4) No error is introduced by cutting off the interaction at six times the disk diameter and it is possible to cut off at half this value without significant loss of precision.

Simulation of the Du Noüy ring surface energy measurement revealed that correct surface energy alone does not lead to minimum energy surfaces and that random particle movements, emulating temperature, are necessary to achieve this goal. With the use of a correction factor and emulated temperature, a fluid with arbitrary surface energy can be simulated by the DEM method.

Simulation of gas hydrate growth in the sediment showed convincing gas hydrate behavior, but also illustrated artifacts that are introduced by representing a 3D world in 2D.

5 Conclusions

A method to simulate a surface tensed medium with DEM is developed and the applicability of this approach is shown with a series of benchmark experiments. Potentials derived from only the nearest neighbors have to be corrected for long-range effects and the application of random particle movement – an equivalent of temperature – was identified as a crucial point for realistic cluster behavior.

There are problems in the restriction to two dimensions that cannot be overcome. However, we think that the proposed method is applicable for moderate gas hydrate volumes and fine grain size.

For a simulation of cementation, it is necessary to move to a 3D simulation, which is perfectly possible with the same implementation strategy. However, a 3D simulation is expected to require more computational power than a 2D simulation for the same number of elements, and the element number will scale with the cube and not the square of the problem size.

We think that other problems in which surface tension is important may benefit from the described method, such as partly saturated soils, multiphase flow, and growth of other concretions in the sediment.

Acknowledgements The initiation and initial funding of DEM modeling of hydrate growth in porous sediments trace back to the work group Ingenieurgeologie at the Institute of Geosciences, Kiel University. Further model development at the Technische Universität Berlin was funded by the German Federal Ministry for Education and Research (BMBF) within the "Geotechnologien" research program "Gashydrate im Geosystem" grant no. 03G0560A. The benchmark experiments and fine-tuning was funded by the DFG – Research Center Ocean Margins (RCOM) of Bremen University (No. RCOM XXXX). We want to thank Lothar te Kamp from Itasca Consultants GmbH for helping with C++ problems during the implementation. The authors are solely responsible for the contents of this paper.

References

1. Sloan, E.D.: Clathrate Hydrates of Natural Gases. Marcel Dekker, Inc., New York, Basel (1998)
2. Mienert, J., Posewang, J., Baumann, M.: Gas hydrates along the northeastern Atlantic Margin; possible hydrate-bound margin instabilities and possible release of methane. In: Henriet, J.P., Mienert, J. (eds.) Gas Hydrates; Relevance to World Margin Stability and Climate Change, pp. 275–291. Geological Society of London, London, UK (1998)
3. Bondevik, S., Harbitz, C.B., Dawson, A., Dawson, S., Løvholt, F., Mangerud, J., Svendsen, J.I.: The Storegga Slide tsunami along the Norwegian coast – from the geological record to numerical simulations. http://www.ibg.uit.no/~stein/abstarct02fig_NPF2002.htm. Cited 12. Mar. 2003 (2002)
4. Bondevik, S., Svendsen, J.I., Johnsen, G., Mangerud, J., Kaland, P.E.: The Storrega tsunami along the Norwegian coast, its age and runup. Boreas **26**, 29–53 (1997)
5. McIver, R.D.: Role of naturally occurring gas hydrates in sediment transport. AAPG Bull. **66**, 789–792 (1982)
6. Winters, W.J., Booth, J.S., Mason, D.H., Commeau, R.F., Dillon, W. P.: Laboratory testing of gas hydrates in marine sediment. American Geophysical Union Spring Meeting, Baltimore, April (1995)
7. Westbrook, G.K., Long, C., Peacock, S., Haacke, R., Reston, T., Zillmer, M., Flueh, E., Foucher, J.-P., Nouzé, H., Contrucci, I., Klingelhoefer, F., Best, A.I., Priest, J.A., Camerlenghi, A., Carcione, J., Rossi, G., Madrussani, G., Gei, D., Mienert, J., Vanneste, M., Buenz, S., Hetland, S., Larsen, R., Habetinova, E., Minshull, T.A., Chand, S., Clayton, C.R.I., Dean, S.: Techniques for the Quantification of Methane Hydrate in European Continental Margins – HYDRATECH – Final Report. (2004)
8. Beauchamp, B.: Natural gas hydrates: myths, facts and issues. C. R. Geosci. **336**, 751–765 (2004)
9. Kennett, J.P., Cannariato, K.G., Hendy, I.L., Behl, R.J.: Methane hydrates in quaternary climate change: the clathrate gun hypothesis. AGU, Washington (2003)
10. Gunn, D.A., Nelder, L.M., Rochelle, C.A., Bateman, K., Jackson, P.D., Lovell, M.A., Hobbs, P.R.N., Long, D., Rees, J.G., Schultheiss, P., Roberts, J., Francis, T.: Towards improved ground models for slope instability evaluations through better characterization of sediment-hosted gas-hydrates. Terra Nova **14**, 443–450 (2002)
11. Feeser, V.: Gashydratbildung in Tiefseesedimenten-Zur Rolle der sedimentmechanischen Prozess-Steuereung. DGMK-Tag.Ber. **9706**, 51–60 (1997)
12. Henry, P., Michel, T., Clennell, M.B.: Formation of natural gas hydrates in marine sediments 2. Thermodynamic calculations of stability conditions in porous sediments. J. Geophys. Res. **104** (B10), 23005–23022 (1999)
13. Clennell, M.B., Hovland, M., Booth, J.S., Henry, P., Winters, W.J.: Formation of natural gas hydrates in marine sediments 1. Conceptual model of gas hydrate growth conditioned by host sediment properties. J. Geophys. Res. **104**(B10), 22985–23003 (1999)
14. Booth, J.S., Winters, W.J., Dillon, W.P., Clennell, M.B., Rowe, M. M.: Major occurrences and reservoir concepts of marine clathrate hydrates: implications and field evidence. In: Henriet, J.P., Mienert, J. (eds.) Gas Hydrates; Relevance to World Margin Stability and Climate Change, pp. 275–291. Geological Society of London, London, UK (1998)
15. Brewer, P.G., Orr, F.M., Friederich, G., Kvenvolden, K.A., Orange, D.L., McFarlane, J., Kirkwood, W.: Deep ocean field tests of methane hydrate formation from a remotely operated vehicle. Geology **25**, 407–410 (1997)
16. Egeberg, P.K., Dickens, G.R.: Themodynamic and pore water halogen constraints on gas hydrate distribution at ODP Site 997 (Blake Ridge). Chem. Geol. **153**, 53–79 (1999)
17. Spangenberg, E., Kulenkampff, J., Naumann, R., Erzinger, J.: Pore space hydrate formation in a glass bead sample from methane dissolved water. Geophys. Res. Lett. **32**(L24301), 1–4 (2005)
18. Spangenberg, E.: Modeling of the influence of gas hydrate content on the electrical properties of porous sediments. J. Geophys. Res. **106**(B4), 6535–6548 (2001)
19. Tohidi, B., Anderson, R., Clennell, M.B., Burgass, R.W., Biderkab, A.B.: Visual observation of gas-hydrate formation and dissociation in synthetic porous media by means of glass micromodels. Geology (Boulder) **29**(9), 867–870 (2001)
20. Sills, G.C., Wheeler, S.J., Thomas, S.D., Gardener, T.N.: Behaviour of offshore soils containing gas bubbles. Géotechnique 41(2), 227–241 (1991)
21. van Genuchten, M.T.: A closed-form equation for predicting the hydraulic conductivity of unsaturated soils. Soil Sci. Soc. Am. J. **44**, 892–898 (1980)
22. Cundall, P.A., Strack, O.D.L.: A discrete numerical model for granular assemblies. Géotechnique **29**, 47–65 (1979)
23. Murariu, V., Svoboda, J., Sergeant, P.: The modeling of the separation process in a ferrohydrostatic separator using discrete element method. In: Shimizu, Y., Hart, R., Cundall, P.A. (eds.) Numerical Modeling in Micromechanics via Particle Methods – 2004, pp. 119–126. Balkema Publishers, Leiden (2004)
24. Kawamoto, H.: Introduction of research and development on electromechanics of electromagnetic particles for imaging technology. In: Shimizu, Y., Hart, R., Cundall, P.A. (eds.) Numerical Modeling in Micromechanics via Particle Methods – 2004, pp. 95–101. Balkema Publishers, Leiden (2004)
25. Yao, M., Anandarajah, A.: Three-dimensional discrete element method of analysis of clays. J. Eng. Mech. **129**(6), 585–596 (2003)
26. Gröger, T., Tüzün, U., Heyes, D.M.: Shearing of wet particle systems – discrete element simulation. In: Konietzky, H. (ed.) Numerical Modeling in Micromechanics via Particle Methods, pp. 65–72. Balkema Publishers, Leiden (2003)
27. I. Itasca Consulting Group: PFC2D Particle Flow Code in 2 Dimensions (Version 3.0 Manual). ICG, Minneapolis (2002)
28. Kreiter, S., Feeser, V., Grupe, B.: Numerical simulation of gas hydrate behavior in marine sediments using PFC2D. In: Shimizu, Y., Hart, R., Cundall, P.A. (eds.) Numerical Modeling in Micromechanics via Particle Methods – 2004, pp. 191–197. Balkema Publishers, Leiden (2004)
29. du Noüy, L.P.: A new apparatus for measuring surface tension. J. Gen. Physiol. **1**, 521–524 (1919)
30. Israelachvili, J.N.: Intermolecular and Surface Forces. Academic Press, London (1991)
31. Kreiter, S., Feeser, V.: Mechanics of growing gas hydrates in marine sediments – numerical simulation of sediment–hydrate interaction. 14. Tagung für Ingenieurgeologie, Kiel, Germany, 26–29.3 (2003)
32. Allen, M.P., Tildesley, D.J.: Computer Simulation of Liquids. Oxford University Press, (1987)
33. Uchida, T., Ebinuma, T., Ishizaki, T.: Dissociation condition measurements of methane hydrate in confined small pores of porous glass. J. Phys. Chem. B **103**, 3659–3662 (1999)

A simulation of gas hydrate growth in marine sediment using the Distinct Element Method - a toolbox for fabric studies

Authors: Stefan Kreiter [a,*], Tobias Mörz [a], Volker Feeser [b], Bernd Grupe [c]

a DFG - Research Center Ocean Margins, Bremen University, P. O. Box 330 440 D-28334 Bremen, Germany

b Institute of Geosciences, Christian-Albrechts-Universität zu Kiel, Hermann-Rodewald-Straße 9 D-24118 Kiel, Germany

c AG WUM, Technische Universität Berlin, Müller-Breslau-Strasse (Schleuseninsel), D- 10623 Berlin, Germany

* Corresponding author: E-mail address: skreiter@uni-bremen.de, Fax: +49 421 218-65810

To be submitted to "Journal of Structural Geology"

Abstract

Gas hydrate bearing sediments have recently been identified as a common part of the marine continental margins. The behavior of gas hydrate bearing sediment is important, because the failure planes of several major and hazardous slope failures at the continental margin lie in gas hydrate influenced sediment. Moreover climatic important carbon releases have been caused by gas hydrate and gas hydrate is a potential future energy resource. The fabric of gas hydrate is a key factor for all three topics. In the first part of the paper natural fabrics of gas hydrate bearing sediment are analyzed.

In the second part the fabric evolution of gas hydrate in sediment is simulated with the Distinct Element Method simulation (DEM). Virtual sediments are composed with fabrics resembling natural host sediments and are adjusted to the same cohesion and angle of friction of natural sediments. In these virtual sediments gas hydrate growth is simulated and the influence of anisotropy and effective stress is analyzed. High anisotropies and high total stress promote layered gas hydrate growth, while low total stress and low anisotropies lead to the growth of nodules. The study is a step to an in depth understanding of gas hydrate growth in marine sediment.

1 Introduction

Gas hydrates are crystalline solids similar to ice, composed of water molecules and small hydrophobic molecules. The most common gas hydrate in nature is methane hydrate (Sloan, 1998). Natural gas hydrates have been discovered first in the permafrost regions of Siberia in 1969 and then in Alaska 1972. Today most of the natural gas hydrate is found around the worlds continental margins at water depth below ~ 300 m.

Generally gas hydrate is stable under high pressure and low temperature and there is a lower boundary of gas hydrate stability in the upper few hundred meters of the sediment. The location of this boundary is mainly dependent on the geothermal gradient and the hydrostatic pressure. A rise in the temperature or a drop in pressure moves this boundary upwards and leads to decay of the gas hydrate. This results in an overall volume increase, because the volume of the emerging methane and water together is much higher than the volume of the equivalent amount of gas hydrate. The volume increase in the pore space reduces the effective stress and may cause slope failure on the continental margin. Several fossil slope failures have been attributed to gas hydrate decay by arguing that the failure plain is coincident with the former base of gas hydrate stability (BGHZ) (Kayen and Lee, 1993; Mienert et al., 1998; Paull et al., 1996) and table 6 in chapter 9 of (Kennett et al., 2003). If the slide following the slope failure is big enough and moves fast enough, a tsunami is generated this is e.g. deduced for the Storegga slide (Bondevik et al., 2002; Bondevik et al., 1997).

Gas hydrate has been identified as an important part of the carbon cycle and the clathrate gun hypothesis claims that methane released from hydrates during slides played a mayor role in the climatic history (Dickens et al., 1997; Kennett et al., 2003). Methane hydrate is regarded as a potential future energy resource (Collett, 2002) and because CO_2 builds also hydrate, there exist plans to store the CO_2 from human fossil fuel consumption on or in the deep sea floor (Lee et al., 2003).

The fabric of the gas hydrate in the sediment is a key factor to understand and predict the behavior of gas hydrate bearing sediment regarding continental slope stability and catastrophic gas releases. A thin unfavorably oriented layer may cause a slope failure, while the same amount of gas hydrate randomly distributed larger nodules does not affect the stability of a continental slope at all. The development of extraction and sequestration strategies also requires knowledge of the fabric development of the sediment. The permeability of the sediment and the accessibility of the gas hydrate is highly dependent on the fabric. Only with a knowledge of the fabric it is possible to exploit gas hydrates in a safe, economic and ecological responsible fashion.

Several geophysical methods are used to detect and characterize gas hydrate bearing sediments, but the same gas hydrate concentration will lead to different measured values depending on the geometric distribution of gas hydrate. Only if the fabric relation of the gas hydrate and the sediment is known, it is possible to interpret the geophysical data like electrical resistivity (Spangenberg, 2001) or p and s wave velocity (Guerin et al., 1999; Korenaga et al., 1997) correctly. The wrong fabric model may lead to incorrect interpretations of gas hydrate concentration and wrong predictions of the sediments behavior.

1.1 Sampling of natural gas hydrates

Gas hydrate bearing sediments are notorious difficult to sample, because of the high pressures and low temperatures needed to conserve the gas hydrates thermodynamic stability. This poses problems during sampling, preservation and further processing of the samples. Standard sedimentological methods for textural analysis like thin sections for microscopy are hard to adapt for samples under high pressures. Even if pressure and temperature are in the stability field of gas hydrates a slight change in effective stress may result in a reorganization of the original structure, since the fabric seems to be dependent on the stress state (Torres et al., 2004). Until now the best samples taken have been pressurized cores form the hydrate ridge

and several shallow lying gas hydrate fields, which have been imaged under pressure with 3D x-ray computer tomography (Abegg et al., 2007; Abegg et al., 2006).

We conclude that gas hydrates are important for several fields of geosciences and that especially the fabric of gas hydrate bearing sediment is of a great importance. This leads to the question of what controls the fabric evolution. In this study we focus on two common gas hydrate fabrics in sediment; nodules and layers and try to distinguish fabric controlling external and internal factors.

Computer simulations are an established approach to complement observations and can partly replace otherwise impossible or expensive experiments. We chose a distinct element method (DEM) simulation to investigate the fabric evolution during gas hydrate growth in marine sediments.

2 Fabric of natural gas hydrate bearing sediments

Natural gas hydrates in sediments have been found in various fabrics. 3D-cements, nodules, veins and layers are common and there is evidence of finely disseminated gas hydrates in clay rich sediments (Abegg et al., 2006; Booth et al., 1998; Ivanov et al., 1998). It is generally accepted that the sediments grain size (Ginsburg et al., 2000; Tohidi et al., 2001) and the stress state (Torres et al., 2004) are factors influencing the development of different fabrics, but a quantitative understanding has not yet been achieved.

Natural gas hydrate fabric was studied in two cores from the Costa Rica continental margin and in an example form the Gulf of Mexico (Fig 1). The gas hydrate bearing specimen in Figure 1a is from the Costa Rica continental margin sampled on the flank of a mud volcano (Flueh et al., 2004). It is interpreted as a bedding parallel gas hydrate layer, probably bound to an ash rich silty layer. Figure 1b is from the same core and shows a thin gas hydrate layer oriented oblique to the bedding. In the left part of figure 1b a dark mafic ash layer crosses the

core and allows to infer the bedding direction, the gas hydrate layer is probably bound to a joint, though other joints with the same direction could not be observed. Figure 1c is from the flank of another mud mound from the Costa Rica margin (Schmidt et al., 2005; Söding et al., 2003) it shows a more complex picture: a jagged vein crosses the core in an oblique angle, and is surrounded by spherical gas hydrate nodules. Here the direction of the bedding is unclear. Figure 1d is a sample for a near surface gas hydrate. It forms thick layers in the near surface sediments, probably parallel to the bedding. Figure 1e shows the differing complex shapes of figure 1c in more detail. The gas hydrate builds round, angular and layered shapes, which lie in near proximity and a general orientation in the direction of the vein structure.

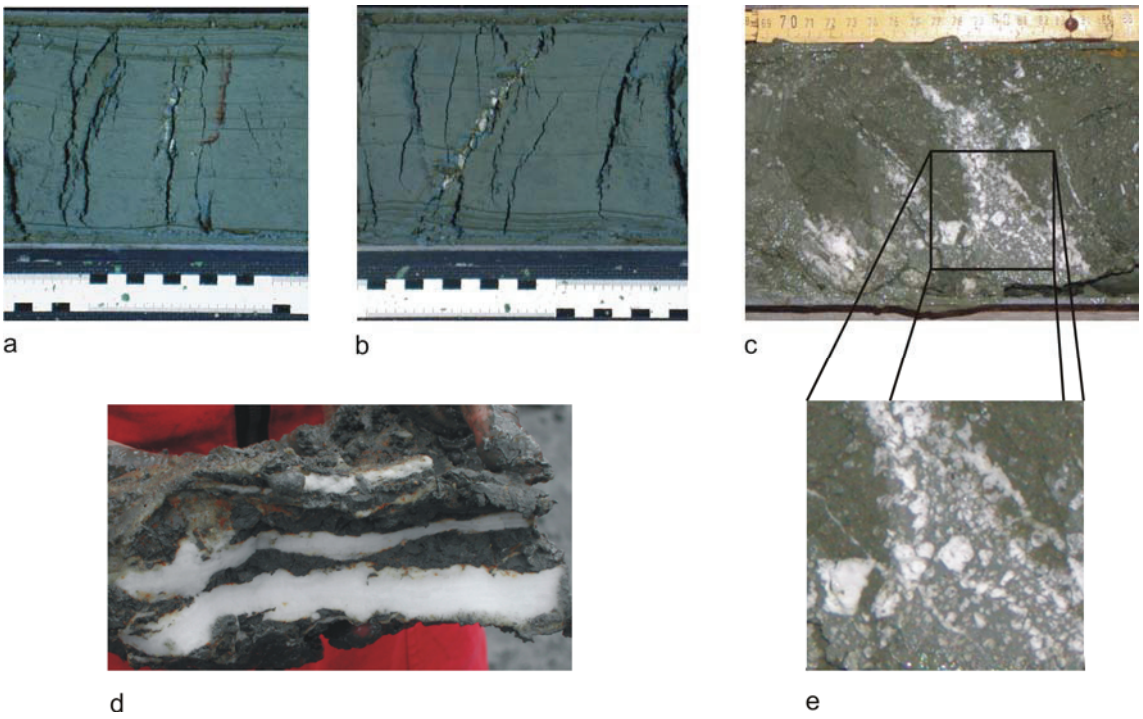

Figure 1.: Examples for fabrics of natural gas hydrates in marine sediment. a) Gas hydrate layer parallel to bedding from 'Mound 12', Costa Rica pacific margin. b) Gas hydrate layer oblique to bedding from 'Mound 12', Costa Rica pacific margin. c) Gas hydrate in nodular and vein like structure from mound 11, Costa Rica pacific margin. d) Massive, layered gas hydrate form Gulf of Mexico, photo F. Abegg Cruise Sonne 174. e) Magnification from c).

It can be concluded that several different fabrics of gas hydrate in sediment are observed in nature. Apparently factors external to the gas hydrate itself will dictate the final morphology, but it is still not clear which external factors are most important and how exactly they influence the growth mechanism.

3 The micro fabric of gas hydrate host sediment

The micro fabric and the pore space geometry of fine grained marine gas hydrate host sediments from ODP leg 164 (Shipboard Scientific Party, 1996) was studied with a scanning electron microscope (SEM)(Fig. 2). During ODP leg 164 chloride anomalies were used as the most secure indicator for gas hydrates. Because sampling for chloride measurements destroys the samples completely, the sediments for structural SEM analysis were sampled in the direct vicinity to the voids left by the pore water sampling. The sediment samples where desalinated, quick-frozen, freeze-dried and broken parallel and perpendicular to the bedding.

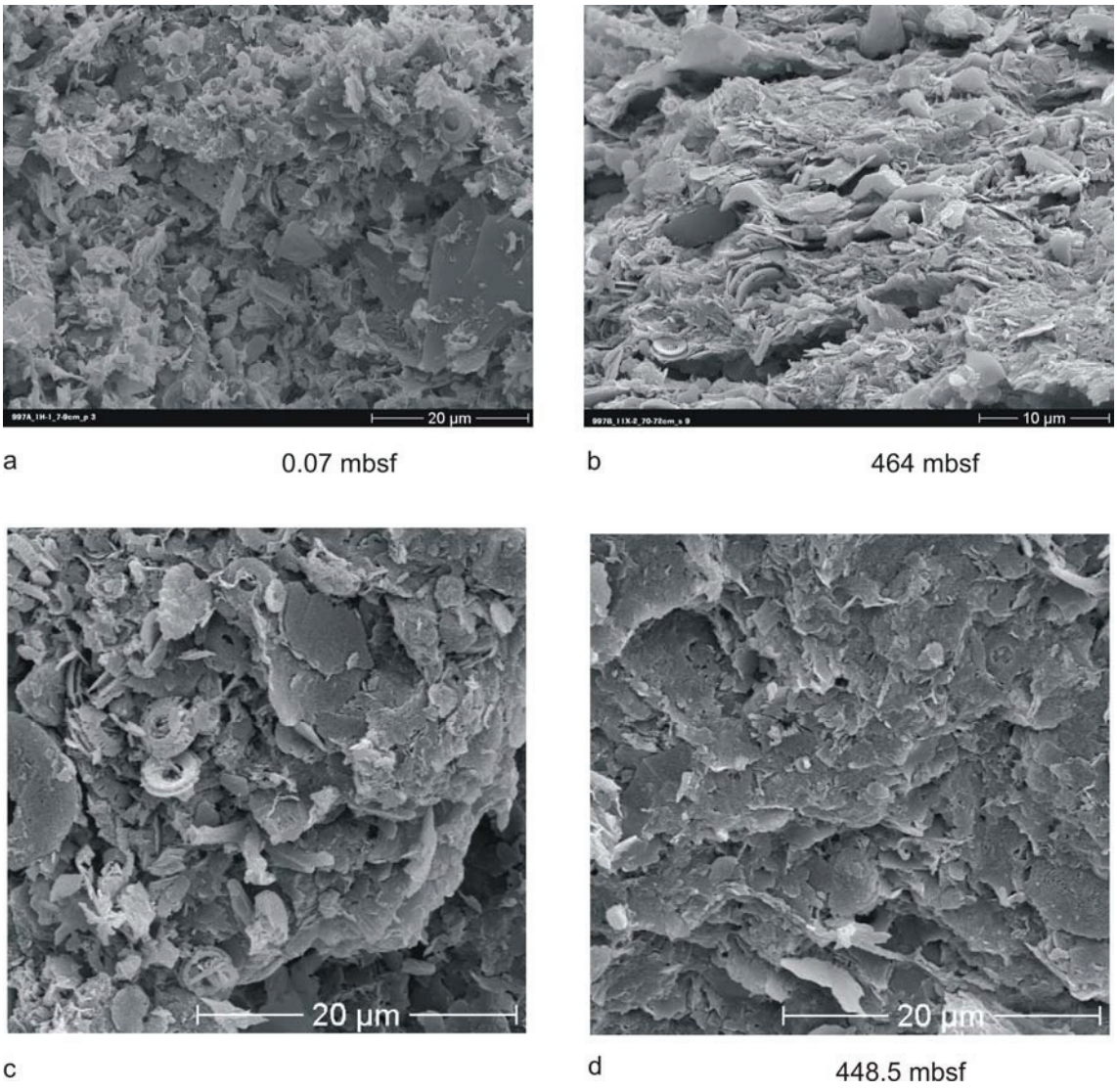

Figure 2.: Scanning electron microscope images from sediment samples from ODP leg 164 hole 997. The depth of the samples is indicated in meters below seafloor (mbsf). Sample **a** was broken parallel to the bedding, sample **b** perpendicular to the bedding and the sample of **c** and **d** also perpendicular to the bedding. Images **c** and **d** are from the same sample.

All SEM images show a mixture of clay minerals, coccoliths and diatom tests and minor amounts of other microfossils and detrital grains. The aim of the micro fabric study was to observe a clear difference in micro fabric between the gas hydrate bearing parts and the gas hydrate free parts of the core. However no clear differences were observed. Only a depth dependent trend could be confirmed: In shallow depth the sediments form a loose structure (fig. 2a), while in deeper parts sediments often show a parallel fabric (fig 2b). The second observation was the micro scale heterogeneity of the sediments. Though the sediments are

uniform to the naked eye the microenvironment is very heterogeneous as illustrated with figures 2 c and d, which are only 0.02 mm apart in the same sample.

4 Methods used for the sediment and gas hydrate simulation.

The Distinct Element Method (DEM) was chosen for the fabric simulation, because its strengths are to simulate the interactions between distinct grains on the scale of single pores. DEM models can simulate arbitrary displacements and free shear failure planes. This is important because natural gas hydrates either grow in faults or veins or displace the neighboring sediments during their growth.

Distinct Element Models are based on freely moving particles which mutually interact. The movement is governed by Newton's laws of motion and the particle interaction forces are modeled by continuous potentials. Gravity, rigid walls, unbreakable bonds, bonds with a given strength and other boundary conditions are used to implement a specific model.

We used the software Particle Flow Code in two dimensions (PFC^{2D}) (Itasca Consulting Group, 2002). PFC is a commercial successor of “Ball” (Cundall and Strack, 1979). This study uses a two dimensional approach, since for the development of a new method calculation speed and also implementation speed is critical.

4.1 The Simulation of the host sediment

The virtual sediments are prepared with the aim to match the fabric of natural clayey samples. The arrangement of the clay-minerals is generated by the compaction processes and is one of the main factors controlling anisotropy of natural samples (fig. 2b).

The geometry of clay particles is approximated by linearly aligned circular particles tied at the contact point forming one unbreakable "clump" (fig. 3). The aligned particles move as one elongated rigid unit, which is the 2D equivalent of a plate (te Kamp and Konietzky, 2003).

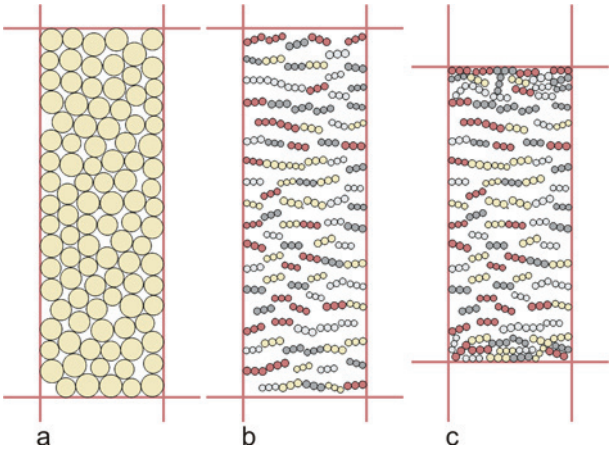

Figure 3.: Illustration of the preparation process of the virtual host sediment with a reduced number of 100 elements: a) equilibrated random distribution of disks. b) State after the replacement of the disks by three aligned, rigid bound particles. The rigid bound elements are plotted in the same color; differing super-particles are colored differently in reddish brown yellow and grays to allow a distinction between them. c) State during the compression/consolidation process.

The particles in natural sediments are randomly distributed in the sense that they do not occur in a regular lattice like atoms in a crystal, but they may have some regularity like a parallel fabric (fig. 2b). To provide such random distributions with the DEM the natural processes which have acted on the sediment, are partly emulated within the simulation (fig. 3).

The particles are assembled in a two stage procedure: In a first step a container is filled with circular particles of slightly varying grain size by the standard material preparation procedure (Itasca Consulting Group, 2002)(fig. 3a). In a second step the random particles are substituted by the aligned particle "clumps", the plates. The plates are randomly oriented with angles of +– 30° to the horizontal orientation (fig. 3b).

Following the generation and orientation of the plates, the sample is compressed in the vertical direction, to mimic the natural compaction process and get the sample adapted to the desired effective stress (fig. 3c). The applied vertical stress is set corresponding to the starting conditions of the following experiment.

After the sample has adapted to this stress state, bonds are installed, which correspond to a complex combination of DLVO- with hydration and structural forces between clay minerals

(Israelachvili, 1991). These forces lead to the cohesion of the clayey sediment. The result is an anisotropic material with a geometry resembling natural sediments (fig. 2b).

4.1.1 Calibration of grain to grain friction (angle of friction) and bond strength (cohesion)

For a realistic simulation the material has to match the natural sediment in terms of geometry, but additionally in terms of bulk properties. Therefore the grain to grain interactions expressed in stiffness, density, bond strength and grain to grain friction have to be chosen appropriately. The relation between the grain to grain interactions and bulk shear strength properties is highly dependent on the actual geometry of the specimen. The grain to grain potentials and friction of clay particles in fact are due to complex quantum mechanical phenomena, which are neither theoretically fully understood nor have they been measured experimentally (Israelachvili, 1991). Following a common solution for this problem in DEM simulations the relation of micro and macro (bulk) properties is established by a series of simulated geotechnical standard lab tests (Giese, 2003).

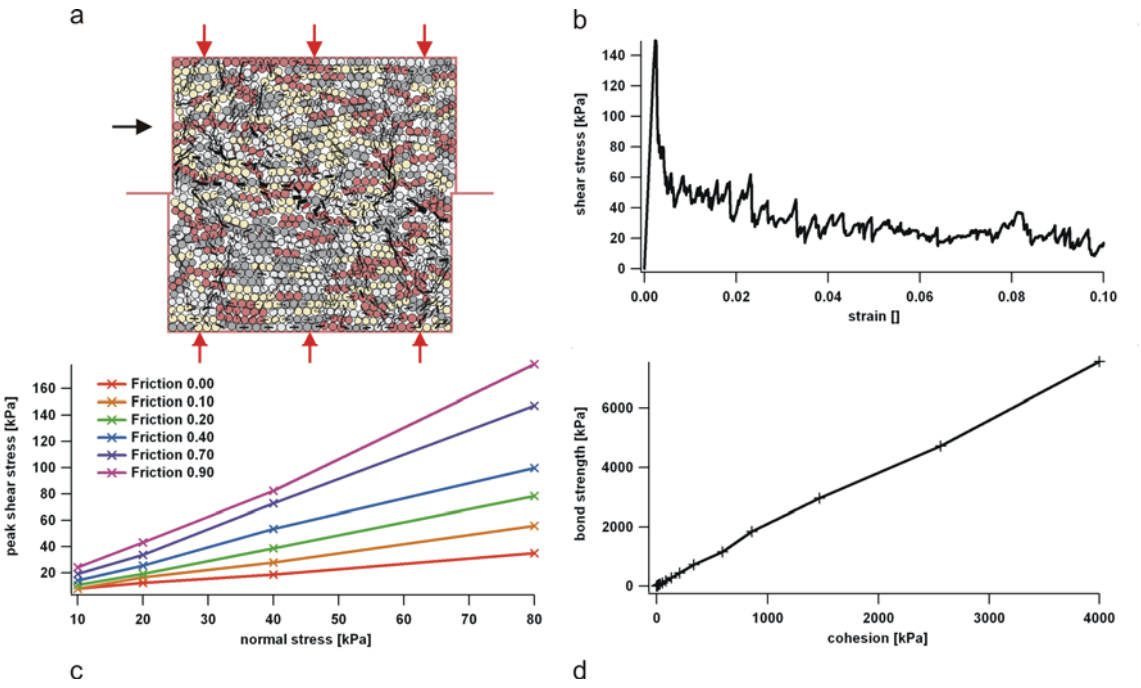

Figure 4.: Characterization of the virtual gas hydrate host sediment. a) virtual shear box during the experiment. Black arrow: direction of movement. Red arrows: controlled constant normal stress. The rigid bound elements are plotted in the same color and the differing particles are colored differently in brown yellow and gray to allow a distinction between them. The lines between the particles indicate direction and magnitude of force between them: black compression, red tension. b) Plot of shear stress vs. strain. c) Result of a series of shear experiments with varying inter particle friction and varying normal stress. d) Micro to macro property relation for one material type.

Several full scale specimens are created and then the boundary conditions from the generation process are replaced by a numerical shear box (fig.4a). The specimen is sheared and the result of such a test is processed like a real laboratory experiment: first the stress strain relationship is plotted (fig. 4b), then the peak shear stresses of different experiments are evaluated (fig. 4c). The final result is a micro to macro property relationship for the tested type of material (fig. 4d). This type of experiment is made for the different virtual materials used in this study.

The shear box experiment is also designed to measure the anisotropy of shear strength by shearing in horizontal or in vertical direction.

The virtual sediment for the growth tests was adjusted to match the bulk properties of known gas hydrate host sediments. The direct assignable grain density was taken from the shipboard measurements (Shipboard Scientific Party, 1996) and the shear strength influencing properties of bonding strength and grain to grain friction were adjusted according to the shipboard

measurements and additional literature (Bartetzko and Kopf, 2007; Lupini et al., 1981; Rizkallah, 2005).

4.2 The simulation of growing gas hydrate

The applied simulation method for gas hydrate is founded on the surface energy. The material is simulated by growing circular particles, an attractive interaction between them, random movements of the particles and particle decay. The particle properties are set up in such a way, that a cluster of them has the same surface energy as a gas hydrate crystal. The attraction and agitation are in fact an upscaling of molecular processes, the growth and decay of the circular particles are a method to allow for smooth growth in an upscaled material. The gas hydrates surface tension is set to 0.039 J/m^2 (Uchida et al., 1999). A detailed description of the simulation technique of gas hydrate growth is given in Kreiter et al., (Kreiter et al., 2007).

The method assumes that the gas hydrate crystals are in thermodynamic equilibrium, that the surface energy governs the mechanical gas hydrate to sediment grain interaction and that the growth process can be simulated much faster if dynamic effects can be excluded. These assumptions are in our opinion applicable and are confirmed by the literature about the thermodynamic constraints on crystal and gas hydrate growth (Becker and Day, 1916; Clennell et al., 1999; Everett, 1961; Feeser, 1997; Fletcher and Merino, 2001; Henry et al., 1999).

4.2.1 Simplifications in terms of kinetics and material transport

This paper is focused on the mechanical interactions in the pore space and the mechanical interaction of a growing crystal determined by the surface energy. Whether a crystal actually grows is determined by the thermodynamic drive and the kinetics. Low temperature, high pressure and super saturation of methane generate the thermodynamic drive in the case of gas hydrate crystal growth. The thermodynamic drive is modified by additional chemicals and the

pore radius (Henry et al., 1999). The kinetics of gas hydrate growth is in general slow and particularly the nucleation of a new gas hydrate crystal is very difficult, even in an open container. In the restrained pore space of the sediment the nucleation of a new crystal is very rare which leads in natural sediments to a high thermodynamic drive for an existing gas hydrate crystal (Henry et al., 1999). Therefore we neglected the thermodynamic drive, which may generally be assumed as high and assume a constant rate of gas hydrate growth.

4.3 Variables and boundary conditions of the gas hydrate growth experiment.

Natural sediments are very variable in terms of physical properties and degree of spatial anisotropy. Natural gas hydrate fabric is also very variable (fig 1). In this study only the in our opinion most important properties are varied, which are the particle length and isotropic effective stress state. Development of the gas hydrate fabric in such a virtual sediment is observed and correlated with the varied parameters.

An anisotropic sediment sample is prepared as described (fig. 3) and a tiny particle is inserted in the middle acting as the gas hydrate crystal nucleus. The nucleus then grows until a given area of the sample cell area is covered with gas hydrate (fig. 5). During the experiments the gas hydrates particle configuration is recorded. The growth velocity is restricted to exclude dynamic effects, the experiment is therefore equivalent to a drained element test.

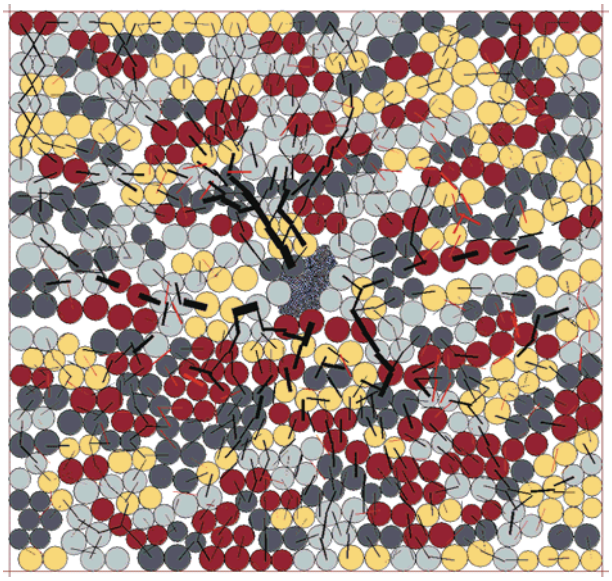

Figure 5: Sediment sample with growing gas hydrate in the center. Gas hydrate simulating particles blue (and tiny). Rigid tied elements have the same color, differing non tied particles are randomly colored in brown yellow and grays. The lines between the particles indicate direction and magnitude of force between them: black compression, red tension.

The growth of the gas hydrate crystal adds volume to the system which results in a reduction of the pore space and an overall volume increase of the sample. The simulation comprises an arbitrary part of the sediment from a slope or a basin. Therefore the walls can set to be rigid or set to a user defined stress, which is subsequently moved to keep this stress level constant to replace the effect of the surrounding sediment. To measure the pure influence of the sediment, for this study the stress is set to a constant value for all boundaries and is only varied between different experiments. But the setup is implemented to be used as a toolbox for different experiments additional to changing stress states and other virtual sediments may be tested.

4.4 aspect ratios

The growing gas hydrate crystal is represented by a multitude of particles and the geometry of such an assembly cannot be compared quantitatively without a standardized procedure. Therefore the ensemble of disks is described in terms of a best fitted ellipse and the geometries of these fitted ellipses are compared with each other (fig. 6).

Figure 6.: Examples for ellipses fitted to a gas hydrate grain configuration. Black areas are the particle locations, inter particle voids are "closed" by image processing.

The difference between a nodule like ellipse and an ellipse equivalent to a layer is best described in terms of aspect ratio R.

$$R = \frac{a}{b} \quad (1)$$

Where **b** is the minor half axis and **a** is the mayor half axis of the ellipse, R varies between 1, which means the ellipse is a circle and infinity if the ellipse degenerates to a line. The development of the aspect ratio is traced over time in a given experiment and this evolution is compared to data from other model runs with different setups.

5 Experiments

5.1 Growth in sediments with parallel fabric

A series of gas hydrate growth experiments is conducted with varying sediment conditions with the aim to get threshold sediment properties discerning between layered and nodular growth. Figure 7 shows the evolution of the aspect ratio with gas hydrate area increase of a part of the conducted experiments. The evolution of the aspect ratio during such a series starts

always with unity, the aspect ratio of the perfect sphere of the gas hydrate seed particle and than proceeds to aspect ratios representing a more or less elongated shape (Fig. 7).

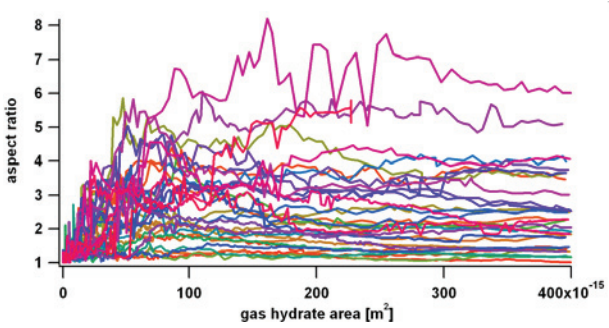

Figure 7.: Evolution of the aspect ratio of the gas hydrate, shown for a part of the experiments with varying particle length and isotropic effective stress.

A part of the experiments evolve to very low aspect ratios and often the aspect ratios start to increase to a value of 2 and then decrease again to the end of the experiment. Another part of the experiments evolves to aspect ratios exceeding 3 and often accompanied by an increase in the end part of the experiment. Aspect ratios above 5 may occur during the experiments, but then the aspect ratios show scatter and may decline after a while.

For the further analysis the aspect ratio at the end of the virtual experiment is taken, to visualize the result of the experiment together with the varying external influence factors (fig. 8).

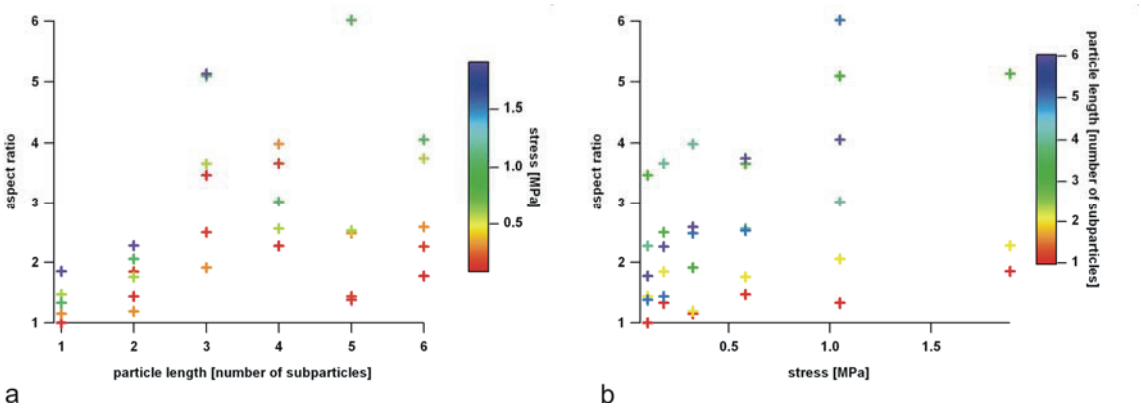

Figure 8.: Final aspect ratios of the experiment series. a) aspect ratio at the end of the simulation over particle length, color of the markers is set to the stress during the experiment. b) Same data as a) results of aspect ratio over the stress during the experiment, here the number of particles is encoded as marker color.

Both plots of figure 8 show enormous scatter, but in both plots there is a trend to higher aspect ratios to higher values of the X axis. This trend is clearer for the particle length than for the stress. Another characteristic of the results can be seen with the help of the color encoding. In both plots the trend becomes much clearer if the red, orange and in b yellow markers are ignored, which corresponds to low values of the color encoded parameter.

6 Discussion

The scatter seen in figure 8 can be explained by the random sample preparation. The virtual sediment is very sensitive to the initial geometry when forming the first crack by gas hydrate growth, which then often controls the further evolution of the gas hydrate fabric (fig. 7). This is a characteristic of granular materials, the forming of a first crack is always random though the process leads to regularities (Hobbs et al., 2004).

The trend seen in Figure 8a is interpreted in the sense, that longer plates lead to high anisotropies and that this high anisotropy is transferred to the guest mineral as final high aspect ratio. Three sub particles per particle are at least needed to get layered growth.

The stress dependency of the high aspect ratios is explained with the surface energy and the supporting of the anisotropy. The surface energy always drives the form towards perfect spheres if no additional forces are applied and in this case the main additional force comes

from the external stress. The second argument is that the anisotropy of the material may be supported by the external stress, the absolute strength difference rises with rising external stress and this is the factor important for the shape of the gas hydrate.

6.1 Comparison with natural gas hydrate fabric.

Most gas hydrate layers are found in a shallow depth, where the stresses are low and where the clay minerals have no distinct parallel fabric (fig. 2a). The simulation would predict for such a scenario nodular gas hydrate growth, while in nature often layers are observed. But not all boundary conditions important for this environment are yet implemented in the simulation. We propose that bedding of cohesive and non cohesive sediments like silty turbitite layers in hemipelagic sediments is most important for this type of environment. The bedding introduces a strong anisotropy in the orientation of the beds as can be seen in figure 1a. Another important factor may be the complex stress states, that can be inferred for the environments where the samples were gained, which are near to a mud volcano or intermittent active methane seeps.

Also the size of the simulation has to be kept in mind, the layer shown in figure 1d is much larger than the whole simulated sample. The sample size was chosen to simulate the clay minerals at the true scale and therefore the gas hydrates simulated here are much smaller than the layers found in situ. For thicker layers the surface energy is less important and low normal stresses are sufficient to form a gas hydrate layer. The layers found in nature have thicknesses up to several centimeters which would necissiate a virtual sample dimension of at least 10 cm. The simulation size in this study is 100 µm, which results in a scaling factor of 10^3. This would raise the computational power needed by at least a factor 10^6, which exceeds the computational power of the largest systems existing today.

The simulation of very high aspect ratios, matches with the observation that in deeper sediment column gas hydrate is often distributed in thin veins (Abegg et al., 2006). The often

vertical orientation however is not yet predicted. The simulation of oblique veins is most probably a result of jointing prior to gas hydrate growth or an anisotropic stress state during the growth of the gas hydrate.

6.2 Analog process: Dyking

Comparable to the growth of gas hydrate in the sediment is in some respects the emplacement of volcanic dykes. Existing anisotropies and the actual stress state control the final geometry of the additional volume in a host material. While textbooks on igneous petrology underline the stress state as the only control of the process (Best, 2003), recent studies argue for the importance of a structural control some mayor dyking events (Jourdan et al., 2006; Valentine and Krogh, 2006). We argue for a similar, but much smaller scale structural control of gas hydrate fabric.

7 Conclusions

- It is possible to set up DEM models to simulate the gas hydrate sediment interaction resulting in the formation of gas hydrate nodules and gas hydrate layers within virtual host sediment.
- Assuming a homogenous material the anisotropy and the effective stress are the main factors influencing the gas hydrate fabric. Anisotropy is recognized as more important than the effective stress.
- The here illustrated method has to be expanded to account for all natural gas hydrate textures, especially gas hydrate cements.
- The introduced simulation techniques may also be used for the simulation of magma ascent and dyke creation.

8 Outlook

The simulation of the fabric of natural gas hydrate bearing sediment is one step to the understanding of the behavior of gas hydrate bearing sediment of continental margins. The final state of the simulations conducted here are to be used for simulations regarding the shear strength of gas hydrate bearing sediment and the shear strength of such a sediment after gas hydrate decay.

Further comparisons with natural gas hydrate samples and with laboratory experiments with gas hydrate bearing sediment are intended, up to now the data base is sparse.

References

Abegg, F., Bohrmann, G., Freitag, J., and Kuhs, W.F., 2007, Fabric of gas hydrate in sediments from Hydrate Ridge—results from ODP Leg 204 samples: Geo-Marine Letters, v. 27, p. 269-277.

Abegg, F., Bohrmann, G., and Kuhs, W.F., 2006, Data report: Shapes and structures of gas hydrates imaged by computed tomographic analyses, ODP Leg 204, Hydrate Ridge, *in* Tréhu, A.M., Bohrmann, G., Torres, M.E., and Colwell, F.S., eds., Proceedings ODP, Scientific Results, 2006: Online, p. 11.

Bartetzko, A., and Kopf, A.J., 2007, The relationship of undrained shear strength and porosity with depth in shallow (< 50 m) marine sediments: Sedimentary Geology

Deformation of soft sediments in nature and laboratory, v. 196, p. 235-249.

Becker, G.F., and Day, A.L., 1916, Note on the Linear Force of Growing Crystals: Journal of Geology, v. 24, p. 313-333.

Best, M.G., 2003, Magma Ascent and Emplacement: Field Relations of Intrusions, Igneous and methamorphic petrology - 2nd ed., Blackwell Science Ltd, p. 210-241.

Bondevik, S., Harbitz, C.B., Dawson, A., Dawson, S., Løvholt, F., Mangerud, J., and Svendsen, J.I., 2002, The Storegga Slide tsunami along the Norwegian coast - from the geological record to numerical simulations.

Bondevik, S., Svendsen, J.I., Johnsen, G., Mangerud, J., and Kaland, P.E., 1997, The Storrega tsunami along the norwegian coast, its age and runup: Boreas, v. 26, p. 29-53.

Booth, J.S., Winters, W.J., Dillon, W.P., Clennell, M.B., and Rowe, M.M., 1998, Major occurrences and reservoir concepts of marine clathrate hydrates: implications and field evidence, *in* Henriet, J.P., and Mienert, J., eds., Gas hydrates; relevance to world margin stability and climate change, Volume 137: Geological Society Special Publications: London, United Kingdom, Geological Society of London, p. 275-291.

Clennell, M.B., Hovland, M., Booth, J.S., Henry, P., and Winters, W.J., 1999, Formation of natural gas hydrates in marine sediments 1. Conceptual model of gas hydrate growth

conditioned by host sediment properties.: Journal of Geophysical Research, v. 104, p. 22985-23003.

Collett, T.S., 2002, Energy Resource Potential of Natural Gas Hydrates: AAPG Bulletin, v. 86, p. 1971-1992.

Cundall, P.A., and Strack, O.D.L., 1979, A Discrete Numerical Model for Granular Assemblies: Géotechnique, v. 29, p. 47-65.

Dickens, G.R., Castillo, M.M., and Walker, J.C.G., 1997, A blast of gas in the latest Paleocene: Simulating first-order effects of massive dissociation of oceanic methane hydrate: Geology, v. 25, p. 259-262.

Everett, D.H., 1961, The Thermodynamics of frost damage to porous solids: Transactions of the Faraday Society, v. 57, p. 1541-1551.

Feeser, V., 1997, Gashydratbildung in Tiefseesedimenten - Zur Rolle der sedimentmechanischen Prozess-Steuereung: DGMK-Tagungsbericht, v. 9706, p. 51-60.

Fletcher, R.C., and Merino, E., 2001, Mineral growth in rocks: kinetic-rheological models of replacement, vein formation, and syntectonic crystallization: Geochimica et Cosmochimica Acta, v. 65, p. 3733-3748.

Flueh, E., Söding, E., Suess, E., and Wallmann, K., 2004, RV-Sonne Cruise Report SO173/1,3&4. Subduction II: The Central American Continental Margin, Volume 115: Kiel, GEOMAR report 115.

Giese, S., 2003, Numerical simulation of vibroflotation compaction - application of dynamic boundary conditions, *in* Konietzky, H., ed., Numerical Modeling in Micromechanics via Particle Methods: Gelsenkirchen, Balkema.

Ginsburg, G., Soloviev, V.A., Matveeva, T., and Andreeva, I., 2000, SEDIMENT GRAIN-SIZE CONTROL ON GAS HYDRATE PRESENCE, SITES 994, 995 AND 997, *in* Paull Charles, K., Matsumoto, R., Wallace Paul, J., and Dillon, W.P., eds., Proceedings of the Ocean Drilling Program, Scientific Results, Volume 164, p. 237-245.

Guerin, G., Goldberg, D., and Meltser, A., 1999, Characterisation of in situ elastic properties of gas hydrate-bearing sediments on the Blake Ridge: Journal of Geophysical Research, v. 104, p. 17781-17795.

Henry, P., Michel, T., and Clennell, M.B., 1999, Formation of natural gas hydrates in marine sediments 2. Thermodynamic calculations of stability conditions in porous sediments: Journal of Geophysical Research, v. 104, p. 23005-23022.

Hobbs, B.E., Ord, A., Regenauer-Lieb, K., Boschetti, F., Zahng, Y., and Durrlemann, S., 2004, Ab initio emergent phenomena in PFC, *in* Shimizu, Y., Hart, R., and Cundall, P.A., eds., Numerical Modeling in Micromechanics via Particle Methods - 2004: Leiden, A. A. Balkema Publishers, p. 191-197.

Israelachvili, J.N., 1991, Internolecular and surface forces: London, Academic Press Limited, 450 p.

Itasca Consulting Group, I., 2002, PFC^{2D} Particle Flow Code in 2 Dimensions (Version 3.0 Manual): Minneapolis, ICG.

Ivanov, M.K., Limonov, A.F., and Woodside, J.M., 1998, Extensive deep fluid flux through the sea floor on the Crimean continental margin (Black Sea), *in* Henriet, J.P., and Mienert, J., eds., Gas hydrates; relevance to world margin stability and climate

change, Volume 137: Geological Society Special Publications: London, United Kingdom, Geological Society of London, p. 195-213.

Jourdan, F., Feraud, G., Bertrand, H., Watkeys, M.K., Kampunzu, A.B., and Le Gall, B., 2006, Basement control on dyke distribution in Large Igneous Provinces: Case study of the Karoo triple junction: Earth and Planetary Science Letters, v. 241, p. 307-322.

Kayen, R.E., and Lee, H.J., 1993, Slope stability in regions of sea-floor gas hydrate; Beaufort Sea continental slope, *in* Schwab, W.C., Lee, H.J., and Twichell, D.C., eds., Submarine landslides; selected studies in the U.S. Exclusive Economic Zone.: U. S. Geological Survey Bulletin: Reston, VA, United States, U. S. Geological Survey, p. 97-103.

Kennett, J.P., Cannariato, K.G., Hendy, I.L., and Behl, R.J., 2003, Methane Hydrates in Quaternary Climate Change: The Clathrate Gun Hypothesis: Washington, AGU, 216 p.

Korenaga, J., Holbrook, W.S., Singh, S.C., and Minshull, T.A., 1997, Natural gas hydrates on the southeast U. S. margin: Constraints from full waveform and travel time inversions of wide-angle seismic data: Journal of Geophysical Research, v. 102, p. 15345-15365.

Kreiter, S., Feeser, V., Kreiter, M., Moerz, T., and Grupe, B., 2007, A Distinct Element simulation including surface tension - towards the modeling of gas hydrate behavior.: Computational Geosciences, v. published online.

Lee, H., Seo, Y., Seo, Y.-T., Moudrakovski, I.L., and Ripmeester, J.A., 2003, Recovering Methane from Solid Methane Hydrate with Carbon Dioxide: Angewandte Chemie International Edition, v. 42, p. 5048-5051.

Lupini, J.F., Skinner, A.E., and Vaughan, P.R., 1981, The drained residual strenght of cohesive soils: Géotechnique, v. 31, p. 181-213.

Mienert, J., Posewang, J., and Baumann, M., 1998, Gas hydrates along the northeastern Atlantic Margin; possible hydrate-bound margin instabilities and possible release of methane, *in* Henriet, J.P., and Mienert, J., eds., Gas hydrates; relevance to world margin stability and climate change, Volume 137: Geological Society Special Publications: London, Geological Society of London, p. 275-291.

Paull, C.K., Buelow, W.J., Ussler, W.I., and Borowski Walter, S., 1996, Increased continental-margin slumping frequency during sea-level lowstans above gas hydrate-bearing sediments: Geology, v. 24, p. 143-146.

Rizkallah, V., 2005, Empfehlungen des Arbeitsausschusses "Ufereinfassungen" Häfen und Wasserstraßen EAU 2004, *in* EAU, ed.

Schmidt, M., Hensen, C., Morz, T., Muller, C., Grevemeyer, I., Wallmann, K., Mau, S., and Kaul, N., 2005, Methane hydrate accumulation in "Mound 11" mud volcano, Costa Rica forearc: Marine Geology, v. 216, p. 83-100.

Shipboard Scientific Party, 1996, Proceedings of the Ocean Drilling Program Volume 164 Initial reports: College Station TX, Texas A&M University.

Sloan, E.D., 1998, Clathrate hydrates of natural gases: New York, Basel, Marcel Dekker, Inc., 705 p.

Söding, E., Wallmann, K., Suess, E., and Flueh, E., 2003, RV-Meteor Cruise Report M54/2+3. Fluids and Subduction Costa Rica 2002, Volume 111: Kiel, GEOMAR report 111.

Spangenberg, E., 2001, Modeling of the influence of gas hydrate content on the electrical properties of porous sediments: Journal of Geophysical Research, v. 106, p. 6535-6548.

te Kamp, L., and Konietzky, H., 2003, Conceptual modeling of Opalinus Clay with FLAC and PFC, *in* Konietzky, H., ed., Numerical Modeling in Micromechanics via Particle Methods: Gelsenkirchen, A. A. Balkema Publishers, p. 315-320.

Tohidi, B., Anderson, R., Clennell, M.B., Burgass, R.W., and Biderkab, A.B., 2001, Visual observation of gas-hydrate formation and dissociation in synthetic porous media by means of glass micromodels: Geology (Boulder), v. 29, p. 867-870.

Torres, M.E., Wallmann, K., Trehu, A.M., Bohrmann, G., Borowski, W.S., and Tomaru, H., 2004, Gas hydrate growth, methane transport, and chloride enrichment at the southern summit of Hydrate Ridge, Cascadia margin off Oregon: Earth and Planetary Science Letters, v. 226, p. 225-241.

Uchida, T., Ebinuma, T., and Ishizaki, T., 1999, Dissociation Condition Measurements of Methane Hydrate in Confined Small Pores of Porous Glass: Journal of Physical Chemistry B, v. 103, p. 3659-3662.

Valentine, G.A., and Krogh, K.E.C., 2006, Emplacement of shallow dikes and sills beneath a small basaltic volcanic center - The role of pre-existing structure (Paiute Ridge, southern Nevada, USA): Earth and Planetary Science Letters, v. 246, p. 217-230.

Conclusion:

This thesis contributes to the understanding of the behavior of gas hydrate bearing sediments, which is amongst others important, because the failure plain of several huge slides on continental slopes are located in gas hydrate influenced sediments. Gas hydrate and the surrounding sediment are simulated with the Distinct Element Method (DEM) and the resulting behavior is examined with various virtual experiments.

The surface energy causes the forces exerted by growing crystals; hence a new method to simulate the surface energy of gas hydrate within the DEM method is proposed and validated. The importance of surface energy in building different shapes of growing new phases in the pore space of sediments with different grain size is shown in a 2D simulation. In numerical experiments the genesis of nodular and layered gas hydrate growth was studied. In this study the impact of parallel fabric of elongated particles and the normal stress on the resulting gas hydrate fabric is shown. It is discussed that gas hydrate "cementation" of pore space can only be simulated in a 3D model. Therefore the proposed method was designed to be also applicable in 3D simulations. A preliminary simulation of gas hydrate decay proves the possibility to expand the method to the whole "lifecycle" of gas hydrate in marine sediment. The simulation of early and late gas hydrate growth revealed a fundamental difference in the resulting principal stress direction.

The work is a first step to the understanding of gas hydrate behavior in the sediment on the way to assess the risk of gas hydrate induced natural hazards at continental margins. The main achievement is a possibility to produce natural fabrics of gas hydrate bearing sediment with the DEM. The resulting virtual samples can be used for studies regarding the strength of gas hydrate bearing sediment of different fabrics along different stress and temperature paths.

The proposed method is not restricted to gas hydrates, but is applicable for other geological problems where surface energy is important like ice growth in soil, multi phase flow in porous media and others.

Outlook:

There are several fields of work which are worth further efforts. My favorite would be to move to a 3D simulation, which would give the simulation a much greater reliability and the possibility to simulate gas hydrate cementation and decay in a more realistic way. Especially the degrees of rotational and positional freedom are only natural in 3D and therewith directly comparable porosities can be simulated. Since 3D simulations require more computational resources the use of high performance parallel computers would be indicated.

A further refinement of the simulation of the host sediment is needed to finally match all laboratory and field experiments done for a certain sediment type.

The coupling of fluid dynamic simulation to gas hydrate growth simulation would open up the possibility to simulate faster processes and include material transfer.

A simulation of gas hydrate decay would be a nice goal, too, however efforts should start after coupled fluid dynamic simulation are implemented.

Also the simulation of dynamic processes like earthquake impact on a partly decayed gas hydrate sample is a future possibility.

It also seems possible to include the thermodynamic drive and a mass balance of methane and water in the model. The simulation of the gas hydrate nucleation kinetics is in my opinion not possible, because of the lack of an accepted model for bulk experiments.

The results are to be compared with laboratory experiments and in situ measurements of gas hydrate bearing sediment. Laboratory data form the geotechnical gas hydrate sediment labs in Germany, Norway and the USA, are currently produced and may in future be compared with the presented simulations.

Danksagung

Vor allem will ich meinen Betreuern Prof. Dr. -Ing. Volker Feeser und Prof. Dr. Tobias Mörz danken. Vielen Dank Herrn Prof. Feeser für die Idee zu dem Thema, die Anschaffung der ersten Software Lizenz, für die Anregungen zur Teilname an interessanten Tagungen und für die stetige Hilfe bei den diversen Publikationen. Danke, Herr Prof. Mörz für die Möglichkeit bei Ihnen zu promovieren, für rege Diskussionen zu dem Thema, für die Hilfe bei den Publikationen und besonders auch für die angenehme Arbeitsatmosphäre die ohne Sie nicht möglich wäre.

Großer Dank gilt Herrn Dipl. geol. Bernd Grupe, der in Berlin meine ersten wissenschaftlichen Arbeiten nach der Diplomarbeit betreute. Als Koordinator des GASSTAB Projekts hat er die Entwicklung des Themas in der Anfangsphase maßgeblich gefördert und mir ermöglicht die im Projekt angeschaffte Software Lizenz in Bremen weiter zu Nutzen. In diesem Zusammenhang will ich Dipl. geol. Michael Maggiulli, Dipl. Ing. Hans-Jürgen Hohnberg und Dipl. Ing. Horst Mudrack für die nette Zusammenarbeit und anregende Diskussionen zum Thema Gashydrat danken. Vielen Dank an Herrn Siegfried Mücke, ohne den viele praktische Teile der Arbeit nicht möglich gewesen wären. Frau Brigitte Schönebeck und Herrn Dr. Hasso Pahlke möchte ich danken für sprachliche und formale Korrekturen an den in Berlin entstandenen Texten.

Bedanken möchte ich mich auch bei den noch nicht erwähnten Mitarbeitern im GASSTAB Verbundprojekt: Prof. Dr. -Ing. Savidis, Herrn Dr. Klaus Hoffmann, Herrn Dr. Hermann J. Becker, und Herrn Dipl. Ing. Jens Schupp, die mich durch ihre Arbeit und ihr Interesse an den geotechnischen Fragen in Zusammenhang mit Gashydrat führenden Sedimenten bei meiner Arbeit motiviert haben und bei Diskussionen über das Thema wertvolle Anregungen gegeben haben.

Vielen Dank an Herrn Dr. Lothar te Kamp von Itasca Consultants GmbH., der mir bei Problemen mit der Software mit Analyse der Fehler, Rat und Tat geholfen hat. Vielen Dank an Herrn PhD. P. A. Cundall, der mir die Anregung gab wie ich den Kontakt-Detektions-Mechanismus von PFC für meine Zwecke nutzen kann.

Mein Besonderer Dank gilt Herrn Dr. Warner Brückmann, Herrn (jetzt Prof.) Dr. Klaus Wallmann und Herrn Prof. Dr. Erwin Suess, die mir ermöglichenden an zwei Ausfahrten des SFB 574 Teilzunehmen und dabei auch tatsächlich Gashydrat zu sehen.

Zu guter Letzt möchte ich mich ganz herzlich bei meiner ganzen Familie bedanken, die mich in jeder Hinsicht bei der Promotion unterstützt hat. Die Unterstützung geschah einerseits durch fachliche Mitarbeit, strategische Tips, Hilfe bei diversen Texten und strenger Projektleitung, aber auch besonders durch Liebe, Verständnis und Aufmunterung.